ChemTexts (2020) 6:26
https://doi.org/10.1007/s40828-020-00117-8

LECTURE TEXT

The hydrophobic effect: is water afraid, or just not that interested?

Todd P. Silverstein[1]

Received: 16 July 2020 / Accepted: 10 September 2020 / Published online: 20 October 2020

Abstract
Our understanding of the hydrophobic effect has advanced greatly since 1990, with the help of experimental, theoretical, and computer simulation results. The key hydrophobic signature of positive ΔC°_{P} and negative ΔS° at room temperature has been interpreted in light of the importance of solvent cavity creation, solvent-excluded volume, and solute–water intermolecular forces, along with some unusual thermodynamic properties of pure water. Application of the hydrophobic effect to the hydration of small nonpolar solutes, protein folding stability, and protein–ligand binding is discussed in detail in this review, with an emphasis on thermodynamic analyses and interpretations.

Keywords Hydrophobic effect · Protein unfolding · Protein stability · Thermophilicproteins

Introduction

The fact that oil and water do not mix is a commonly observed outcome of the hydrophobic effect. It is hard to overestimate the importance of this effect in real-world chemistry and biochemistry: The cleaning action of soaps and detergents, the influence of surfactants on surface tension, chromatographic separation (reverse-phase), the formation of lipid membranes and micelles, partitioning across membranes (e.g., the blood–brain barrier) and the bioavailability of drugs and toxins, the folding and stability of proteins and their ability to bind hydrophobic ligands are all based in large part on the tendency of nonpolar groups to aggregate in aqueous solution. It is thus not surprising that this has been an area of intense study for more than a century.

In 1998 I published a paper in the *Journal of Chemical Education* entitled "The real reason why oil and water don't mix" [1]. In this paper I pointed out that all undergraduate general and organic chemistry textbooks got it wrong when they attempted to explain why oil and water don't mix. All of these texts claimed that the process of transferring a nonpolar solute into water is endothermic, due to the necessity of breaking water–water hydrogen bonds in order to create a cavity for the solute. In fact, it has been known since at least the 1940s that this process is exothermic at room temperature, hence the reason why oil and water don't mix is because of the negative entropy change upon hydration of the nonpolar solute. One simply cannot attempt to explain this phenomenon without addressing water's loss of motional freedom.

In preparing to write this updated review of the hydrophobic effect for *ChemTexts*, I consulted a large number of general and organic chemistry textbooks published since 2005; imagine my disappointment that with one notable exception [2], all of the textbooks still purveyed the same error. One book even attempted to somehow mitigate the erroneous information by referring students to my 1998 paper for "more background in thermodynamics than we have thus far been able to provide." There is no reason to include in textbooks an explanation that has been known for 8 decades to be wrong! Either supply the correct explanation or avoid an explanation entirely. The purpose of this review is to apprise students, instructors, and textbook writers of the great strides that have been made since 1990 in understanding the hydrophobic effect. In particular, I will concentrate on thermodynamic parameters and calculations, stressing changes in enthalpy, entropy, free energy, and heat capacity.

To begin, we must first define what we are studying [3]. Many terms have been used to modify the word hydrophobic: effect, interaction, force, bond, factor. Hydrophobic effect is perhaps the most general of the terms, and it is often used to cover the whole panoply of phenomena listed above

✉ Todd P. Silverstein
tsilvers@willamette.edu

[1] Department of Chemistry (Emeritus), Willamette University, Salem, OR 97301, USA

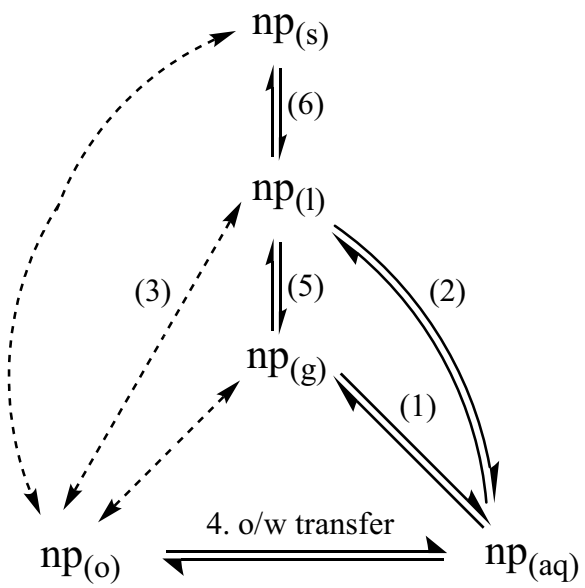

Fig. 1 A nonpolar (np) solute can be transferred into aqueous solution from three different initial phases: (1) from the pure gas phase, hydration; (2) from the pure liquid phase, neat transfer; or (4) from solution in an organic solvent, oil/water (o/w) transfer. A fourth transfer is possible for large nonpolar solutes, from the pure solid phase; this would entail either fusion (6) followed by neat transfer, or organic solvation followed by o/w transfer. Modified from ref. [3]

[4]. Hydrophobicity is often studied in two very different laboratory systems: the hydration of small nonpolar solutes, and the folding and unfolding of large polymers (e.g., proteins, detergent micelles) that are at least partly hydrophobic. One of the most surprising and satisfying aspects of hydrophobic theory is that models developed to explain the former simple system can be successfully applied to the latter complex polymer system (but see [5]). The driving force for the polymer folding/assembly process is often called the hydrophobic force.

The transfer of a nonpolar solute into aqueous solution is actually three (or four) different processes, which must be distinguished. The differences between these processes can be clarified in a thermodynamic cycle diagram (Fig. 1). Process 1, hydrophobic hydration (Yaminsky and Vogler [6] pointed out the oxymoronic nature of this term!) is the simplest process thermodynamically, because the initial nonpolar phase can be treated as an ideal gas, with no appreciable intermolecular forces. For this reason, a few authors have expressed a clear preference for studying this process [7–9]. The problem is that when extrapolating results to complex polymer systems, the initial nonpolar phase there is more akin to a liquid, or possibly even a solid [10]. Starting from appropriate standard states (identical number density or molar concentration, e.g., 1 M), both neat/water (reaction 2 in Fig. 1) and oil/water transfer (o/w, reaction 4) are quite similar,[1] and are both studied extensively in the literature. The term hydrophobic interaction is usually reserved for the spontaneous aggregation of nonpolar solutes in aqueous solution, i.e., the reverse of neat/water transfer.

Note that neat transfer (process 2 in Fig. 1) can be viewed as the sum of vaporization (process 5) and hydration. Because ΔH° and ΔS° for vaporization are positive and fairly large, there is a substantial difference between hydration and neat transfer. Using *n*-butane as an example (Table 1), we see that the signs of ΔH° and $298{\cdot}\Delta S^\circ$ (negative), and ΔG° (positive) are the same for both processes, but the magnitudes are smaller for neat transfer (especially so for ΔH° and $T\Delta S^\circ$). For this reason, one of the more frustrating aspects of the hydrophobicity literature is that authors are not always careful to specify which of the three processes (hydration, neat transfer, or oil/water transfer) they are studying [3].

Before we move on, it is a good idea to flesh out the relationship between the two laboratory systems mentioned above: (i) transfer of small nonpolar solute into aqueous solution vs. polymeric unfolding/disassembly/release. Table 2 specifies the reactants and products for each of these processes. Reaction (ii) represents the disassembly of a lipid bilayer or detergent micelle into aqueous monomers; reaction (iii) the release of a bound ligand from a protein receptor; and (iv) the denaturation of a folded (native) protein. In each reaction, the reactants are two separate phases, water plus an aggregated nonpolar phase, and the product is a single mixed phase: hydrated nonpolar groups in aqueous solution. Insights gathered from the simplest system (i), aqueous solubility of small nonpolar solutes, have been successfully

Table 1 Thermodynamic parameters at 25 °C for *n*-butane hydration, vaporization, and neat transfer (= vaporization + hydration)

	ΔH° (kJ/mol)	$298{\cdot}\Delta S^\circ$ (kJ/mol)	ΔG° (kJ/mol)	ΔC°_P (J/K/mol)
Vaporization	+ 23.0	+ 24.5	− 1.5	− 43
Hydration	− 23.6	− 32.3	+ 8.7	+ 390
Neat transfer	− 0.6	− 7.8	+ 7.2	+ 347

Hydration data: ref. [11]; vaporization: NIST

[1] ΔH and ΔS for reaction (3) are approximately zero [3].

Table 2 Nonpolar (np) neat transfer and related biochemical reactions

	np segregated/aggregated (2 separate phases)	**mixed** (1 phase)	**examples**
(i)	np(o*)	np(aq)	Oil and water don't mix Non-wettable (hydrophobic) surface Drug partitions into/across membrane Toxins bioaccumulate in fat/membrane Reverse phase chromatography
(ii)	PL(bilayer)	PL(aq monomer)	self-assembly of membrane bilayer
	Detergent (micelle)	Detergent(aq)	self-assembly of detergent micelle
(iii)	P·ligand(np)	P(aq) + np(aq)	Ligand (np) binding to receptor
(iv)	P_N (native)	P_U (unfolded)	protein unfolding/folding

*'*o*' "oil" phase, e.g., pure np liquid, organic solvent, or membrane bilayer interior, *np* nonpolar solute, *PL* phospholipid, *P* protein

applied to the more complex systems, membrane bilayer and micelle assembly (ii), ligand–receptor binding equilibria (iii), and protein stability and denaturation (iv).

Thermodynamics of nonpolar solute aqueous solubility

The butane aqueous solubility data in Table 1 are a good place to begin a discussion of hydrophobic hydration and aqueous transfer. The thermodynamic signature of these processes includes the substantial negative ΔS° at room temperature, the negative ΔH° at room temperature (large magnitude for hydration but small magnitude for neat and o/w transfer), and the very large positive ΔC_P. To give a frame of reference for the latter, pure water's moderate heat capacity, 76 J/K/mol, is increased about sixfold by the dissolution of butane. Of course, the fact that ΔC_P is large and positive means that ΔH° and ΔS° for the dissolution process, which are both negative at room temperature, become positive at higher temperatures. Thus for these two parameters there will be a temperature (T_H and T_S, respectively) at which they are zero. From the definition of heat capacity change,

$$\Delta C_P^\circ = \left[\frac{\partial \Delta H^\circ}{\partial T}\right] = T\left[\frac{\partial \Delta S^\circ}{\partial T}\right], \tag{1}$$

(partial derivatives at constant P).

we can integrate to obtain the temperature dependence of ΔH° and ΔS°:

$$\Delta H^\circ(T) = \Delta H^\circ\left(T_{\text{ref}}\right) + \Delta C_P^\circ\left(T - T_{\text{ref}}\right) \tag{2}$$

$$\Delta S^\circ(T) = \Delta S^\circ\left(T_{\text{ref}}\right) + \Delta C_P^\circ \cdot \ln\left(T/T_{\text{ref}}\right). \tag{3}$$

T_{ref} is typically 298.15 K (25.00 °C), but it can be any temperature for which ΔH° and ΔS° have been measured. In fact, from the definition of T_H and T_S, we can also write:

$$\Delta H^\circ(T) = \Delta C_P^\circ \cdot \left(T - T_H\right) \tag{4}$$

$$T_H = T_{\text{ref}} - \Delta H^\circ\left(T_{\text{ref}}\right)/\Delta C_P^\circ \tag{5}$$

$$\Delta S^\circ(T) = \Delta C_P^\circ \cdot \ln\left(T/T_S\right) \tag{6}$$

$$T_S = T_{\text{ref}} \cdot e^{\left(-\Delta S^\circ(T_{\text{ref}})/\Delta C_P^\circ\right)}. \tag{7}$$

Applying Eqs. (2)–(7) to the Gibbs free energy equation ($\Delta G^\circ = \Delta H^\circ - T\Delta S^\circ$), we get

$$\begin{aligned}\Delta G^\circ(T) &= \Delta H^\circ\left(T_{\text{ref}}\right) - T\Delta S^\circ\left(T_{\text{ref}}\right) + \\ &\quad T\Delta C_P^\circ\left(1 - T_{\text{ref}}/T + \ln\left(T_{\text{ref}}/T\right)\right) \\ &= T\Delta C_P^\circ\left(1 - T_H/T + \ln\left(T_S/T\right)\right).\end{aligned} \tag{8}$$

So, if one knows ΔC°_P and two other parameters, either $\Delta H^\circ(T_{\text{ref}})$ and $\Delta S^\circ(T_{\text{ref}})$, or T_H and T_S, one can calculate ΔG° at any temperature.

Using the butane data in Table 1 and Eqs. (2)–(8), we can plot ΔG°, ΔH°, and $T\Delta S^\circ$ as a function of temperature

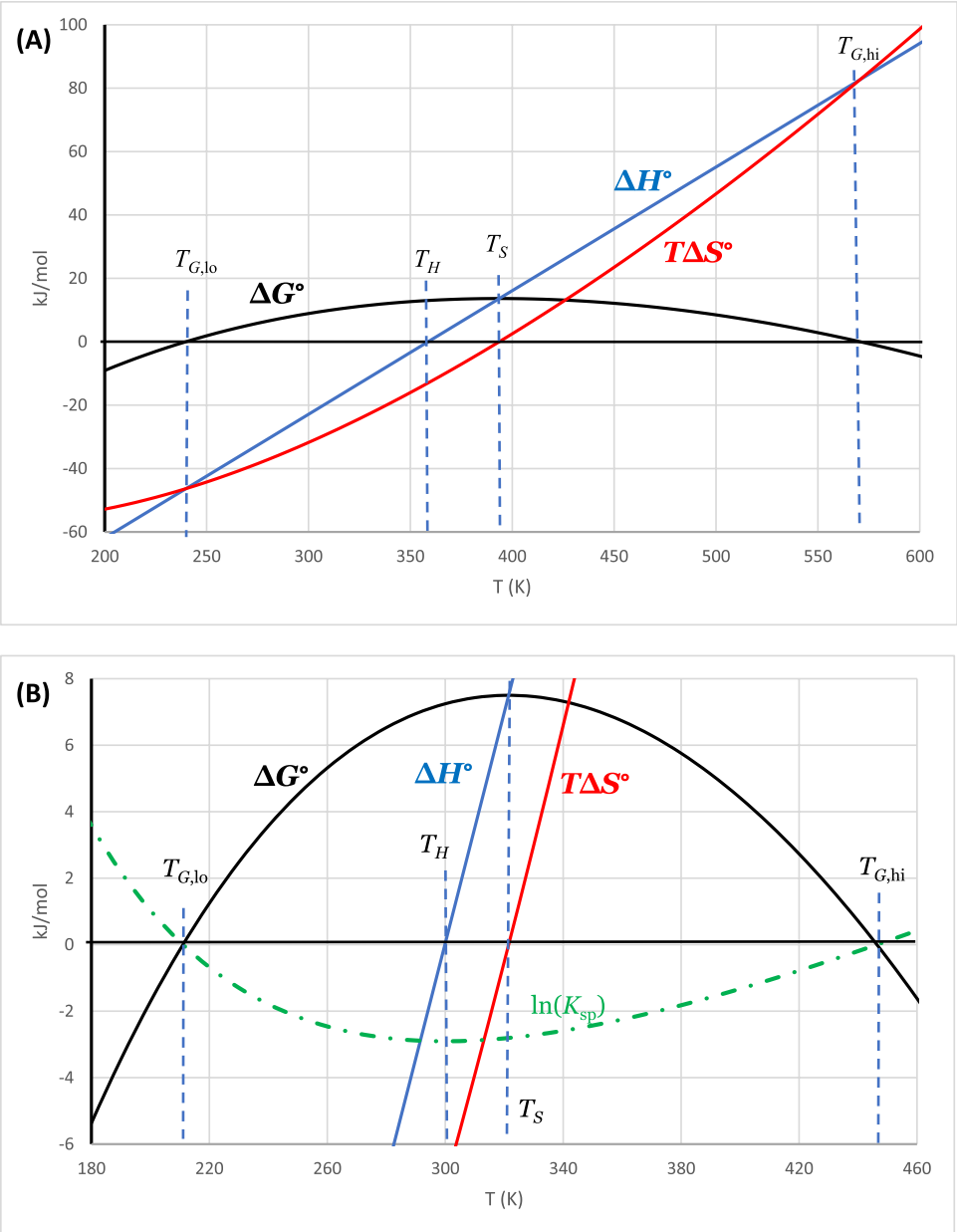

Fig. 2 $\Delta G°$ (black curve), $\Delta H°$ (blue curve), and $T\Delta S°$ (red curve) as a function of temperature for butane **a** hydration and **b** neat transfer. The green dashed curve plots $\ln(K_{sp})$ vs. T. ΔC_P is assumed to be temperature independent in these plots (In fact, ΔC_P decreases slightly with increasing temperature up to ≈ 400 K, then rises dramatically above 520 K, as the critical temperature of water is approached [12].)

(Fig. 2). $\Delta H°$ increases linearly with T, with slope = ΔC_P. As with most small nonpolar solutes, for neat transfer (Fig. 2b), T_H is close to room temperature, and T_S is near 50 °C (323 K).[2] The $\Delta G°$ vs. T curve resembles an upside-down parabola, which crosses the T-axis at two points, $T_{G,lo}$ and $T_{G,hi}$; at these two points, $\Delta H° = T\Delta S°$. $T_{G,lo}$ and $T_{G,hi}$ depend only on T_H and T_S; using Eq. (8) and setting $\Delta G°(T) = 0$, we can derive that they are the two temperatures that satisfy the following equation:

$$1 - T_H/T + \ln(T_S/T) = 0. \tag{9}$$

$\Delta G°$ reaches a maximum[3] at T_S, because the slope of the $\Delta G°$ vs. T curve is zero at the maximum, and $\partial\Delta G°/\partial T = \Delta S°$. From Eq. (8), the maximum value of $\Delta G°$ is

[2] Sets of related compounds (e.g., noble gases, alkanes, benzene derivatives, and even proteins) are believed to demonstrate enthalpy and entropy convergence, at $T_{H,conv}$ and $T_{S,conv}$, temperatures at which all members of the set have the same values of hydration (or o/w transfer) enthalpy or entropy, respectively. These temperatures are distinct from T_H and T_S. Further discussion can be found in the Appendix.

[3] In the older literature, some authors measured and plotted the temperature dependence of the solubility equilibrium constant (e.g., Ostwald partition coefficient) instead of $\Delta G°$ vs. T. As seen in Fig. 2b, the $\ln(K_{sp})$ vs. T curve crosses the T-axis at the same points, $T_{G,lo}$ and $T_{G,lo}$, but reaches its minimum value at T_H, not T_S. This occurs because the slope of the $\ln(K_{sp})$ vs. T curve is zero at the minimum, and $\partial\ln(K_{sp})/\partial T = \partial(\Delta G°/T)/\partial T = \Delta H°/T$.

$$\Delta G^{\circ}_{\max} = \Delta G^{\circ}(T_S) = \Delta C^{\circ}_P \cdot (T_S - T_H). \quad (10)$$

Although butane dissolution in water is nonspontaneous over a wide temperature range, it is important to realize that butane is in fact water-soluble below $T_{G,\mathrm{lo}}$ and above $T_{G,\mathrm{hi}}$. Furthermore, below T_H the reaction is exothermic, so the key force behind the insolubility is the negative ΔS°; however, above T_S, ΔS° is positive, so the key force must be the endothermicity of the reaction. This suggests that the structure of the aqueous butane solution varies dramatically with temperature. This is of course reflected in the large positive ΔC_P, which is the key hallmark of the hydrophobic effect.

Hydrophobicity and solute size

It is well known that water solubility decreases with the size of the nonpolar solute. For example, methanol and ethanol are completely miscible with water, butanol is moderately soluble, and octanol is immiscible. It turns out that hydrophobicity thermodynamic parameters are linearly proportional to solute size. For example, for the hydration of alkanes at 25 °C, ΔH° increases by 0.8 kcal/mol/C, $298{\cdot}\Delta S^{\circ}$ decreases by 0.94 kcal/mol/C, and ΔC_P increases by 13.5 cal/K/mol/C [12–15]. This is an important aspect of hydrophobicity, because it means that large molecules with many hydrophobic groups, (e.g., proteins, polymers) can have very large values of ΔC_P for unfolding (cf., o/w transfer).

While on the subject of size, there is a distinct difference between hydrophobicity observed at the macroscopic vs. microscopic level. If we compare the wetting of large hydrophobic surfaces to the o/w transfer of small nonpolar solutes, ΔC_P is positive in both cases, but room temperature ΔH° and ΔS° are both positive for the macroscopic surface [16], whereas they are negative for small solutes. This macroscopic surface behavior is sometimes referred to as a "nonclassical" hydrophobic effect. From this we can conclude that there is a solute size above which insertion into water causes the breakage of water H-bonds, leading to a rise in both enthalpy and entropy. This in turn leads to the conclusion that there is a crossover radius below which the room-temperature structure and thermodynamics are microscopic (entropy-driven/classical), and above which they are macroscopic (enthalpy-driven/nonclassical). Although many theoretical studies have placed this crossover radius at 4–10 Å [16–23], experimental measurements on large aqueous solutes have yet to confirm nonclassical behavior.[4] For example, alkyl carboxylic acids up to 21 carbons long [26], C_{60} fullerenes [27], graphene sheets [28], hydrophobic polymers [29], and protein surfaces all behave like small solutes rather than macroscopic surfaces. Classical hydrophobicity seems to apply in aqueous solution, no matter the size of the solute.

Solvation = cavity creation + solute/solvent interaction

In order to interpret what thermodynamic results tell us about the nature of the hydrophobic effect, we can model dissolution as a two-step process: first create a cavity in the solvent, then insert the solute and "turn on" solute–solvent interactions. Cavity creation involves not just clearing out an empty space that excludes water, but also reorganizing the water molecules in the shell surrounding the cavity. In other words,

$$\Delta G^{\circ}_{\mathrm{cav}} = \Delta G^{\circ}_{\mathrm{reorg.}} + \Delta G^{\circ}_{\mathrm{excl.vol.}} \quad (11)$$

As mentioned above, most undergraduate chemistry textbooks assume that cavity creation is endothermic because reorganization of the shell waters requires the breakage of water–water hydrogen bonds. However, it has been known for 30 years or more that for nonpolar solutes of small to moderate size, water H-bonds do not have to be sacrificed when creating a cavity [16]. Basically, the water molecules can maintain something close to the H-bonding network found in bulk water by reaching "around" the empty space in the cavity.

Recent evidence [30–37] suggests that while the waters surrounding the hydration cavity have somewhat fewer H-bonds than those in the bulk (3.0 vs. 3.6 per water), these shell H-bonds are slightly stronger (10.8 vs. 9.8 kJ/mol) [31, 32]. Although this adds up to a net loss of stability in the shell ($3.0 \times 10.8 = 32.4$ kJ is less than $3.6 \times 9.8 = 35.3$ kJ), Lee and Graziano have shown that this loss of enthalpy is exactly compensated by a gain in entropy: The loss of bonds is accompanied by a gain in freedom of motion. We will discuss this enthalpy–entropy compensation in more detail below, but for the sake of this discussion, we can write:

[4] A nonclassical hydrophobic effect (ΔH-driven, rather than ΔS-driven) has been observed for large nonpolar solutes that are transferred into water from the pure solid phase (as opposed to the liquid or vapor phase) [24, 25].

$$\Delta G^{\circ}_{\text{reorg.}} = \Delta H^{\circ}_{\text{reorg.}} - T\Delta S^{\circ}_{\text{reorg.}} \approx 0. \quad (12)$$

On the other hand, because the cavity is an excluded volume within which water cannot venture, this decrease in mobility causes a decrease in entropy (when $T < T_S$; a brief discussion of the effect of volume restriction on entropy can be found in the Appendix) [38]. Because all of the enthalpy changes in the cavity creation process are included in the water reorganization term (i.e., $\Delta H^{\circ}_{\text{excl.vol.}} = 0$), and $\Delta G^{\circ}_{\text{reorg}} \approx 0$ (Eq. 12), then for the net process of cavity creation we can write:

$$\Delta G^{\circ}_{\text{cav}} \approx \Delta G^{\circ}_{\text{excl.vol.}} = \Delta H^{\circ}_{\text{excl.vol.}} - T\Delta S^{\circ}_{\text{excl.vol.}} = -T\Delta S^{\circ}_{\text{excl.vol.}}. \quad (13)$$

Regarding solute–solvent interactions, in water these would be dipole–induced dipole intermolecular forces (IMFs), sometimes referred to in the literature as a Lennard–Jones or van der Waals force [12]. Inducing a dipole in a nonpolar molecule (i.e., polarizing the molecule) depends on size: the larger the nonpolar molecule, the more polarizable it is, and the stronger IMFs it will experience in water. Because the solute is already restricted to remain within the cavity, "turning on" IMFs does not appreciably affect entropy [22], so

$$\Delta G^{\circ}_{\text{IMF}} = \Delta H^{\circ}_{\text{IMF}} - T\Delta S^{\circ}_{\text{IMF}} \approx \Delta H^{\circ}_{\text{IMF}} \quad (14)$$

Summing Eqs. (13) and (14), for hydrophobic hydration and neat or o/w transfer we get:

$$\Delta G^{\circ} = \Delta G^{\circ}_{\text{IMF}} + \Delta G^{\circ}_{\text{cav}} \approx \Delta H^{\circ}_{\text{IMF}} - T\Delta S^{\circ}_{\text{excl.vol.}} \quad (15)$$

It is worth noting that $\Delta H^{\circ}_{\text{IMF}}$ and $\Delta S^{\circ}_{\text{excl.vol}}$ are both negative, and they both increase in magnitude (i.e., get more negative) with the size of the nonpolar solute. This relates directly to our observation above that hydrophobicity thermodynamic parameters are proportional to solute size.

What is special about water and nonpolar solutes?

Now is a good time to ask a few important questions about the hydrophobic effect: (1) is water special? And if it is, then what makes it so? (2) Are nonpolar solutes special? Do they differ from polar and ionic solutes?

Is water special? Yes and no (see refs. [39, 40] for excellent reviews on water in biological systems in general, and the hydrophobic effect in particular). In a number of ways, water is like any other solvent. The solvation process begins with cavity creation, with its entropic penalty, no matter the solvent. Thus, the dissolution process is only spontaneous if the solute–solvent IMFs outweigh the ΔS_{cav} penalty (as well as, for neat and o/w transfer, the cohesive forces of the initial nonpolar phase). It turns out that organic solvents are in fact surprisingly good solvents for both nonpolar and polar solutes. Moderately polar liquids like ethanol, propanol, and acetone (dielectric constant (ε) = 20–25) are freely miscible with all organic solvents, as well as water. More polar liquids like methanol, acetonitrile, dimethylformamide, and dimethyl sulfoxide (ε = 30–50) are miscible with all but a few organic solvents (exceptions: pentane, hexane, heptane). Water is called the "universal solvent" because it solvates polar compounds and some salts. But organic solvents solvate nonpolar compounds and some polar ones as well. Perhaps organic solvents should also be considered "universal"!

Because solvent–solute IMFs for nonpolar solutes in organic solvent are weak induced dipole–induced dipole forces (also known as London dispersion forces, LDFs), it seems surprising that organic liquids are such good solvents. This brings up a key difference between water and organic solvents, namely, cohesive forces [41]. Strong cohesive forces in a liquid are reflected in a high density (ρ), surface tension, melting point, boiling point, and vapor pressure, as well as a high isobaric thermal expansion coefficient ($\alpha_P = [\partial \ln\rho/\partial T]_P$), and/or a low isothermal compressibility ($\kappa_T = [\partial \ln\rho/\partial P]_T$). It stands to reason that the cavity-creation work to incorporate a solute is lower for liquids with weaker cohesive forces. Thus, organic liquids, due to their weak cohesive forces, do not require strong solute–solvent IMFs in order to favor solubility.

In addition to its strong cohesive forces, water is unusual in another important respect: it is a very small molecule compared to other liquid solvents [39, 41, 42]. Because of its small size, the probability of finding an empty cavity large enough to accommodate a solute is lower than it would be for other solvents [43–47]. In other words, ΔS_{cav} is large and negative in water for two distinct reasons: its strong cohesive forces and its small molecular size.

Besides its strong cohesive forces and small size, water is unusual in a few other ways [39, 40]. Most prominently, its liquid phase is denser than its solid phase, and its liquid density continues to increase with temperature for several degrees above the melting point, after which density falls. So, unlike most liquids, water has a temperature of maximum density. This, and the fact that the thermodynamics of hydrophobic hydration depend primarily on the ratio α_P/κ_T (also known as the thermal pressure coefficient, $\tilde{p}$) account for most of the unique aspects of aqueous solutions. Specifically, for pure water, $\tilde{p}$ increases dramatically with temperature, whereas it decreases slightly with temperature for most other pure solvents [19, 48, 49]. As we will discuss further below, this trend alone has been incorporated into a powerful model that successfully predicts water's density maximum, as well as the large positive ΔC_P, minimum

solubility temperature, and negative ΔH° and ΔS° of hydrophobic hydration [48–50].

The answer to the second question (are nonpolar solutes special?) is also, perhaps unsurprisingly, yes and no. There are many polar compounds and salts that dissolve in water endothermically (and with positive ΔS°_{soln}): examples include most sugars (e.g., glucose, sucrose), polar amides (e.g., urea, guanidinium chloride), and potassium, sodium, and ammonium salts. But there are just as many that, like nonpolar solutes, dissolve in water exothermically (and with negative ΔS°_{soln}): examples include most molecular gases (e.g., NH_3, H_2S, CO_2), acids (e.g., HCl, H_2SO_4, HNO_3, $HClO_4$, CH_3COOH), as well as most calcium, lithium, and hydroxide salts.

In 1981, Cabani et al. published an important paper in which they used linear free energy relationships to estimate the contributions to ΔH°_{hydrn}, ΔS°_{hydrn}, and $\Delta C^\circ_{P,hydrn}$ of various organic functional groups [51]. In agreement with values discussed above, Cabani et al. found ΔH°_{hydrn} to be slightly negative for nonpolar groups (from − 2.4 kJ/mol for $–CH_3$, to − 6.6 kJ/mol for C=C); for polar groups, the magnitudes were much larger (from − 23 kJ/mol for C=O, to − 60 kJ/mol for O=C–NH_2). This increased exothermicity is due to the stronger water–solute IMFs, both hydrogen bonding and dipole–dipole forces. On the other hand, the separation between polar and nonpolar groups was not as distinct for ΔS°_{hydrn}. The groups with highest polarity had values of $298{\cdot}\Delta S^\circ$ that ranged from − 9 kJ/mol for $–NH_2$ and –OH, to − 14 kJ/mol for N. However, other polar groups (including C=O, –COO, and –COOH) had lower $298{\cdot}\Delta S^\circ$ values that overlapped with those of most nonpolar groups, ranging from − 1 to − 5 kJ/mol.

The results of Cabani et al., along with those of a number of other authors [52–54], allow us to conclude that a major difference between hydration of polar vs. nonpolar solutes lies in the strength of the IMFs. The entropic work of cavity creation is nearly identical for both types of solutes, so the main reason why polar solutes dissolve in water and nonpolar ones do not is that polar solutes enjoy stronger IMFs with water.

A key lesson here is that a negative value of ΔH°_{hydrn} or ΔS°_{hydrn} at room temperature does not distinguish hydration of nonpolar from polar solutes. The factor that does distinguish hydrophobic solvation is heat capacity; as discussed above, ΔC_P is large and positive for nonpolar groups (from + 45 kJ/mol for C, to + 101 kJ/mol for C=C), whereas it is large and negative for polar groups (from − 37 kJ/mol for –COO, to − 87 kJ/mol for O=C–NH–) [51, 52]. Thus, any successful theory of hydrophobicity must explain, first and foremost, the large positive ΔC°_P for hydration and transfer of nonpolar aqueous solutions.

Heat capacity and the hydrophobic effect

Molar heat capacity is defined as the amount of heat that must be added to a mole of substance in order to increase its temperature by one degree (units = J/K/mol). It can be quite different (especially for a gas) if the sample is allowed to expand during heating (constant pressure, isobaric = C_P) or not (constant volume, isochoric = C_V). Pressure is constant in most biochemical systems, so C_P is most relevant. For most chemical substances, C_P is lowest for the gas phase and highest for the liquid phase.

For an ideal gas, C_P depends only on the number of degrees of freedom (f) of the gas particle:

$$C_P = (1 + f/2)R \tag{16}$$

A monatomic gas has only three degrees of freedom (three translational directions), so $C_P = 2.5R = 20.8$ J/K/mol. Polyatomic gases can convert absorbed heat into rotational and vibrational energy, in addition to translational energy, so they have more degrees of freedom that can absorb heat. Thus, more heat must be added to attain a one-degree temperature increase, and polyatomic gases have higher heat capacities than monatomic gases (Table 3).

Solids have higher molar heat capacities than gases, even though solids have very little translational freedom of motion. This is more than made up for by the strong IMFs that hold molecules in a solid together. In solid matter, a good portion of absorbed heat is converted into vibrational energy within these IMF "bonds", so more heat is required to raise the temperature. To understand this effect better, it is convenient to introduce the formal definition of isobaric heat capacity [30]:

$$C_P = \left[\frac{\partial H}{\partial T}\right]_P = T\left[\frac{\partial S}{\partial T}\right]_P. \tag{17}$$

According to Eq. (17), solids (and liquids) have higher heat capacities (than gases) because they are better able to raise their enthalpy and entropy as temperature increases, due to their strong IMFs. Essentially, the IMFs afford more vibrational modes to store the added energy.

Liquid molecules, in addition to strong IMFs, have much more rotational and translational freedom of motion than solids, so liquids generally have the highest heat capacities (Table 3, Fig. 3). On average, C_P(l) is just over twice C_P(g), whereas C_P(s) is about 50% higher than C_P(g), as can be seen in Fig. 3.

The heat capacities of liquid water and water vapor are unremarkable, but solid ice has an unusually low heat capacity; it is essentially identical to that of steam (Fig. 3, black lines). This is probably related to one of the water anomalies mentioned above, the fact that ice is less dense than liquid water. This loose packing in ice means that frozen water molecules are not as close as they are in liquid water, hence IMFs in the solid are not as strong as they could be, and C_P is anomalously low.

Table 3 Molar heat capacities of selected gases, liquids, and solids

Gases		Ideal gas	Liquids		Solids		Dulong–Petit
1-atom							
Noble gases	20.8–21	20.8[a]			Metals	24–29.4	24.9[d]
2-atom							
N_2, H_2, O_2, CO	28.9–29.1	29.1[b]	N_2	39			
			O_2	39			
HCl, HI, Cl_2, Br_2	34–36.4	37.4[c]	HCl	62	HCl, HI, Br_2, I_2	48–54	
			HI	69			
			Br_2	76			
			I_2	81			
3-atom							
H_2O, CO_2, SO_2, N_2O, (CH_4)	36–39	37.4[c]	SO_2	86	CO_2, SO_2	70	
			H_2O	76	H_2O	38	
			CH_4	53			
> 3-atom							
NH_3	29		NH_3	77	NH_3	49	
C_6H_6	82		C_6H_6	136	C_6H_6	129	
n-C_7H_{16}			n-C_7H_{16}	225	n-C_7H_{16}	146	

[a] $f = 3$ (translational) degrees of freedom; $C_P(g) = 2.5R = 20.8$ J/K/mol

[b] $f = 3$ (translational) + 2 (rotational) degrees of freedom; $C_P(g) = 3.5R = 29.1$ J/K/mol

[c] $f = 3$ (translational) + 2 (rotational) + 2 (vibrational) degrees of freedom; $C_P(g) = 4.5R = 37.4$ J/K/mol

[d] Einstein–Dulong–Petit rule: $C_P(s)$ for metals (monatomic) $= 3R = 24.9$ J/K/mol

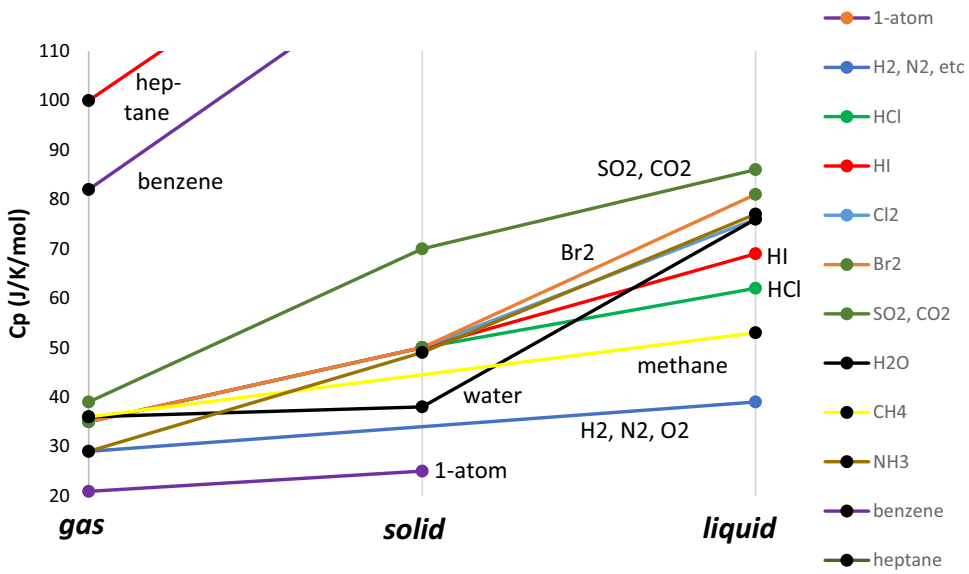

Fig. 3 Molar heat capacity increases with the number of atoms in a molecule, and also with phase: $C_P(g) < C_P(s) < C_P(l)$. Note the anomalously low $C_P(H_2O(s))$

Models of hydrophobic hydration: iceberg vs. water cavity

The large increase in heat capacity upon dissolution of nonpolar solutes in water (e.g., for butane, a sixfold increase) has been reported in the literature since at least 1935 [55], but how can we explain it? What causes the enthalpy and entropy of the solution to rise so dramatically with increasing temperature upon insertion of nonpolar solute into water?

Before we discuss specific structural models of hydrophobic hydration, an interesting non-structural thermodynamic model was proposed by Muller in 1990 [31]. This two-state mixture model envisions every water H atom as either making an H-bond or not, with f being the fraction of

broken H-bonds. (For example, if two specific water molecules in a collection have one of the four H atoms not participating in an H-bond, then $f = 0.25$.) Furthermore, in an aqueous solution, there are assumed to be only two distinct phases: bulk water, and the hydration shell of the nonpolar solute. The process of breaking an H-bond is accompanied by a $\Delta H°$, $\Delta S°$, $\Delta G°$, and K_{eq} that are different in the two phases. Using standard thermodynamic definitions and a few simplifying assumptions, Lee and Graziano [32] came up with a model that successfully accounts for all of the key aspects of hydrophobic hydration. The model predicts that for small nonpolar solutes (e.g., methane to pentane [32]): f increases from 0.1 ± 0.05 (that is 3.4–3.7 H-bonds per water molecule) in bulk water, to 0.25–0.28 in the hydration shell; $\Delta H°$ for breaking an H-bond increases from 9.8 (in the bulk) to 10.8 kJ/mol in the hydration shell, so hydration shell H-bonds are stronger; $\Delta S°$ (H-bond breaking) increases from 21.6 (in the bulk) to 27.5 J/K/mol in the hydration shell, so hydration shell H-bonds have less freedom of motion.

The $\Delta C°_P$ for hydrophobic hydration is accurately predicted by this model, within 0.04% of the experimental value [32]. As a nonpolar solute is added to water, bulk waters must enter the hydration shell; this model predicts that some H-bonds will break (about $3.6 - 3.0 = 0.6$ per hydration shell water), but the hydration shell H-bonds will be stronger (by 1 kJ/mol) and the entropy of the hydration shell waters will decline (by 6 J/K/mol). A number of reports have supported the existence of stronger H-bonds in the hydration shell [30, 33–37, 56]. It is notable that Muller's model accurately accounts for the ΔH, ΔS, and ΔC_P of hydrophobic hydration without making any assumptions at all about the structure of the hydration shell, and without utilizing any physical aspects of the water solvent (e.g., size, density, compressibility, etc.).

Two hydrophobic hydration structural models have been proposed over the years, both dealing with the cavity created in water to accommodate the nonpolar solute; the older and more well-known model is easier to visualize physically, whereas the newer model derives from theory (e.g., scaled particle theory, information theory, integrated equation of state). What the newer model lacks in ease of visualization, it makes up for in the amount of support that it has garnered from experiments and computer simulations.

In 1945, Frank and Evans proposed the "iceberg" model to explain the key thermodynamic aspects of hydrophobic hydration: large negative $\Delta S°$ (and $\Delta H°$) at room temperature, and large positive $\Delta C°_P$. In this model, water molecules at the surface of the cavity created to accommodate the nonpolar solute arrange themselves so that H-bonds are not lost. Key aspects of the structure of this hydration shell are preservation (and perhaps even increase) of the number and/or strength of H-bonds per water molecule, an increase in the tetrahedrality of the H-bond network, and a decrease in freedom of motion of these waters. Such an enhanced structure in the hydration shell would explain the increase in heat capacity. Frank and Evans posited that this hydration shell structure resembled the tetrahedral network found in ice, although they cautioned not to take the "iceberg" analogy too literally. And with good reason, because as we have seen above, the heat capacity of ice is in fact lower than that of liquid water. Over the next 35 years, authors developed this model further [14, 57–63], and terms like flickering cluster and clathrate cage were introduced to replace the "iceberg".

Harnessing experiment, theory, and computer simulations (both molecular dynamics and Monte Carlo), researchers have searched for decades for evidence of the "iceberg", i.e., enhanced structure and reduced mobility in the hydration shell of nonpolar solutes. Until 2007, evidence supporting the existence of such structures was modest at best [30, 32, 42, 64–67]. Since then, the amount of research demonstrating clathrate-like structure in the nonpolar solute hydration shell has mounted steadily [34–36, 68–75]; at the same time, others have failed to observe such structures [33, 37, 76–79]. Furthermore, of the 18 publications citing evidence for the existence of clathrate-like hydration shells, only seven are based on experimental (mostly spectroscopic) results; the rest utilize computer models of water that all have certain drawbacks, and are, by definition, not "real" water.

Summing up the state of the "iceberg" research at this point, it seems likely that although such semi-ordered hydration shell structures do exist, they are probably not extensive enough to account for the large values of $\Delta S°$ and $\Delta C°_P$ that characterize the hydrophobic effect. Interestingly, Joel Hildebrand[5] had already made this point 40–50 years ago! For example, he found that methane's diffusion coefficient was 40% lower in water than in carbon tetrachloride [64]. He concluded that although this decline in mobility was interesting, it could not be explained by the existence of clathrate cages, because these would lower diffusion by one or two orders of magnitude [64].

By creating models of a water-like solvent that featured strong cohesive forces without any tetrahedral hydrogen bonding, some authors have questioned the importance of clathrate cages, which require water's tetrahedral hydrogen-bonding network [41, 80–82]. That they were able to reproduce the key characteristics of hydrophobic hydration with such "Lennard–Jones" solvents led these authors to conclude that hydrogen bonding, and thus clathrate-like hydration shells, are not strictly required to explain the hydrophobic effect.

[5] An American physical chemist (1881–1983) who specialized in solution chemistry and "won virtually every major prize in the field of chemistry except the Nobel Prize".

Lee and Graziano made a similar point, but from a thermodynamic perspective, invoking the concept of enthalpy–entropy compensation [32, 77, 83, 84]. Qualitatively, it is well known that ΔH and ΔS usually have the same sign: Processes that require heat input (positive ΔH, e.g., breaking bonds, melting, boiling) usually also increase freedom of motion (positive ΔS). Lee and Graziano took this a step further, arguing that any reorganization of solvent structure that caused a decrease in enthalpy would incur an exactly compensating decrease in entropy (see also [52]). In other words, $\Delta H_{\text{reorg}} = T\Delta S_{\text{reorg}}$; therefore the structural reorganization could not have a net effect on the overall ΔG for the hydration process. One aspect of such enthalpy–entropy compensation can be seen in Fig. 2b: note that over the temperature range 0–80 °C, the slopes of the $\Delta H°$ vs. T line (blue) and the $T\Delta S°$ vs. T curve (red) are essentially the same. So, any structural change induced by rising temperature raises $\Delta H°$ and $T\Delta S°$ by roughly the same amount, and therefore $\Delta G°$ varies very little over this temperature range. In other words, butane is insoluble in water (positive $\Delta G°$) not because of any special structure in the hydration shell, but because of a disparity between $\Delta H°$ and $T\Delta S°$ that exists at room temperature and remains essentially unchanged up to 500 K (Fig. 2a). This could not be explained by an ordered clathrate-like structure, because such a structure must "melt" away as the temperature rises.

The source of this disparity, as proposed by Lee and Graziano and many others, is the solvent-excluded volume within the water cavity. As explained above, any time one creates a cavity in matter, the loss of mobility lowers entropy [38]; if this cavity can be created in water without sacrificing hydrogen bonds [16], then $\Delta H_{\text{cav}} \approx 0$, and $\Delta G_{\text{cav}} \approx -T\Delta S_{\text{cav}}$. Scaled particle theory has been used successfully to explore the effects of solvent and solute size and shape on ΔS_{cav} [16, 20, 22, 23, 46]. A key lesson from these studies is that ΔS_{cav} scales with the probability of finding a suitably sized cavity in the solvent, so ΔS_{cav} gets more negative as the solute gets bigger, and the solvent gets smaller. From this perspective, the main contribution of water to the hydrophobic effect is its small size and strong cohesive forces. This conclusion is corroborated by the Lennard–Jones solvent results discussed above.

Recently, a few authors have concluded that the signature increase in $\Delta C°_P$ for hydrophobic hydration is a result solely of the unusual properties of pure water, rather than its properties as a solvent [48, 49]. Specifically, water's thermal pressure coefficient ($\tilde{p} = \alpha_P/\kappa_T$) increases steeply with temperature; it is zero at 4 °C, water's temperature of maximum density, and below 4 °C becomes negative. For organic liquids (e.g., benzene) and many other solvents, $\tilde{p}$ decreases slightly with temperature. $\Delta C°_P$ for hydrophobic hydration turns out to be large and positive because $\Delta C°_P$ depends predominantly on $(\partial\tilde{p}/\partial T)_P$ [48, 49].

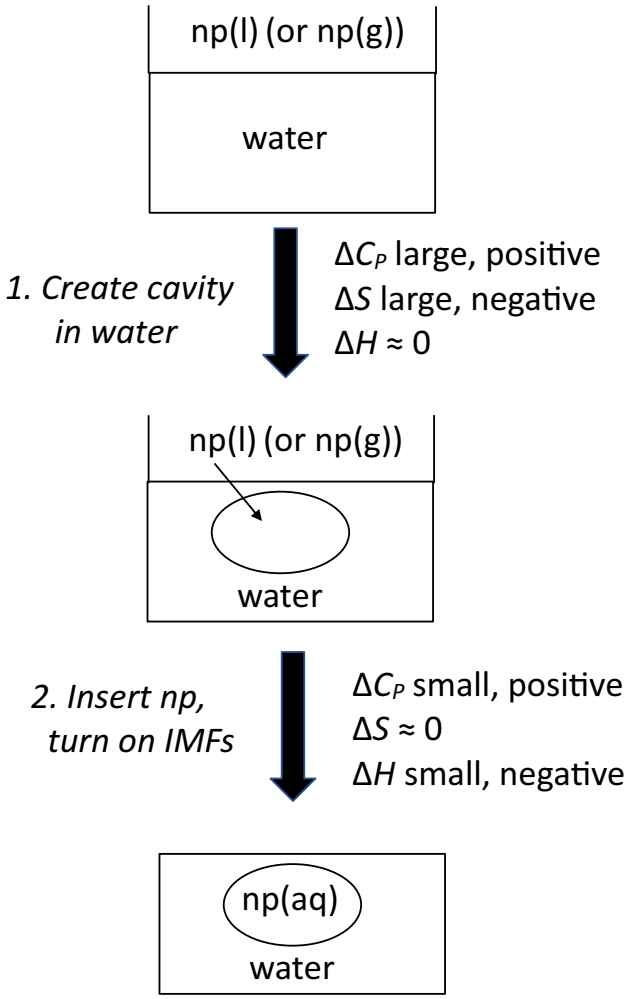

Fig. 4 Summary of the key steps in hydrophobic hydration and neat transfer. np nonpolar solute, IMFs dipole–induced dipole intermolecular forces

It is a good idea to summarize at this point key aspects of the hydrophobic effect learned in the last 30 years. For hydrophobic hydration and o/w transfer below T_H, $\Delta H°$ and $\Delta S°$ are both negative, with $\Delta H° \approx \Delta H°_{\text{IMF}}$, and $\Delta S° \approx \Delta S°_{\text{excl.vol}}$. Additionally, $\Delta C°_P$ is large and positive, due to water's thermal pressure coefficient ($\tilde{p}$) and its unusual temperature dependence. To think about this structurally without the "crutch" of the "iceberg" model, consider Eq. (1): ΔC_P is large and positive if ΔS rises steeply (i.e., becomes less negative) with T. In turn, this occurs because the reorganization of water–water H-bonds upon nonpolar solute insertion allows more freedom of motion with increasing T (personal communication from reviewer). Finally, because of the positive $\Delta C°_P$, above T_H and T_S, $\Delta H°$ and $\Delta S°$ (respectively) become positive.

Figure 4 summarizes the key steps in hydrophobic neat transfer (or hydration), along with their associated thermodynamic parameters. The two main explanatory models

Table 4 Percentage of water-exposed surface area covered by various types of groups in the average globular protein. From ref. [87]

	Nonpolar (%)	Peptide (%)	Polar (%)	Charged (%)	All (%)
Native	57	13	11	19	100
Unfolded	58	13	20	9	100
ΔWASA(U)[a]	58	13	25	4	100

[a]ΔWASA(U) refers to the newly exposed surface area upon unfolding

explain the thermodynamics thusly: According to the iceberg model, the hydration shell waters surrounding the cavity have clathrate-like bonding (positive ΔC_P) and restricted motion (negative ΔS). According to the water/cavity model, the cavity's solvent-excluded volume restricts the motion of water (negative ΔS), and the temperature dependence of water's thermal pressure coefficient accounts for the positive ΔC_P. Results from theory and molecular dynamics simulations suggest that the water/cavity model is the most strongly supported of the two models.

Before we leave this topic of the hydration of small nonpolar solutes, it is worth reconsidering the term "hydrophobic", and the fear vs. indifference notion called out in the title of this paper. Early in the history of hydrophobicity studies, Joel Hildebrand opposed this term, pointing out that since hydrophobic hydration was in fact exothermic, it was misleading to claim that nonpolar solutes "feared" water in any way [64]. Recall that polar and charged solutes dissolve in water because their strong IMFs (dipole–dipole and charge–dipole, respectively) overcome the negative entropy of cavity creation. From this perspective, nonpolar solutes are insoluble in water because their IMFs, though attractive, are simply not strong enough to balance the negative ΔS_{cav}. In other words, nonpolar solutes do not "fear" water. Rather, they are not sufficiently attracted to the solvent; they are "just not that interested".

Protein stability and the hydrophobic effect

The burial of nonpolar side chains in the protein interior, away from the external aqueous solution has been understood since at least 1939 as an important driver of protein folding and stability [85]; Kauzmann,[6] in an influential paper published 20 years later, strengthened this case [58]. By 1990, in light of key papers by Dill [86] and Spolar/Record [87], the hydrophobic force was widely believed to be the most important factor stabilizing protein structure. One of the key arguments raised by nearly all of these authors was that ΔC_P for protein unfolding is always large and positive, just as it is for hydrophobic o/w transfer. The fact that ΔC_P for the hydration of polar groups is negative suggested that the protein folding/unfolding equilibrium is driven mainly by hydrophobic forces and not polar interactions. More recent studies have amended this view, concluding that proteins are stabilized about equally by both hydrogen bonding and hydrophobic forces [88, 89] (but see [5]).

The topology of globular proteins is sometimes naively envisioned as being entirely polar/hydrophilic on the external surface and nonpolar/hydrophobic in the packed interior. This turns out to be incorrect; because of the heterogeneity of the amino acid sequence, with nonpolar and polar groups somewhat evenly distributed, the burial of nonpolar side chains in the protein interior is invariably accompanied by the burial of nearby polar and charged groups [90]. In fact, 83% of all nonpolar atoms (side chains plus alpha carbons) and 82% of all polar peptide groups (O=CR–NH–) are buried together in the protein interior, along with 63% of all polar side chains and 54% of all charged groups [91]. If we consider a typical globular protein to be a 100-Å-diameter sphere, then the interior volume (90 Å diameter) is 73% of the total. Thus, nonpolar atoms and peptide groups are both enriched in the interior by 10 percentage points, whereas polar side chains and charged groups are underrepresented in the interior by 10 and 19 percentage points, respectively.

Alternatively, we can look at the water-accessible surface area (WASA) of the average globular protein, which decreases substantially as the protein folds into its native conformation [38]. As seen in Table 4, the average protein's WASA is almost 60% nonpolar, in both the native and unfolded forms. The surface area that is buried upon folding (−ΔWASA(U)) is not especially enriched in nonpolar groups (or peptides); rather, it is poor in charged groups and enriched in polar groups (Table 4). So, two key distinguishing characteristics of the external surface are that it is enriched in charged groups, but also features nonpolar patches; the interior, on the contrary, is enriched in both nonpolar and peptide groups, whereas charged groups are underrepresented.

Even though the protein interior contains polar and charged groups, the lack of water along with the enrichment of nonpolar groups makes the interior function as a low dielectric medium ($\varepsilon \approx 6$–7; [92]), similar to the organic solvents ethyl acetate and diethyl ether. (The surface is more polar, though not nearly as polar as water: $\varepsilon \approx 20$–30 [92], similar to acetone and methanol.) From Coulomb's law

[6] Walter Kauzmann (1916–2009), an American biophysical chemist, specialized in protein folding.

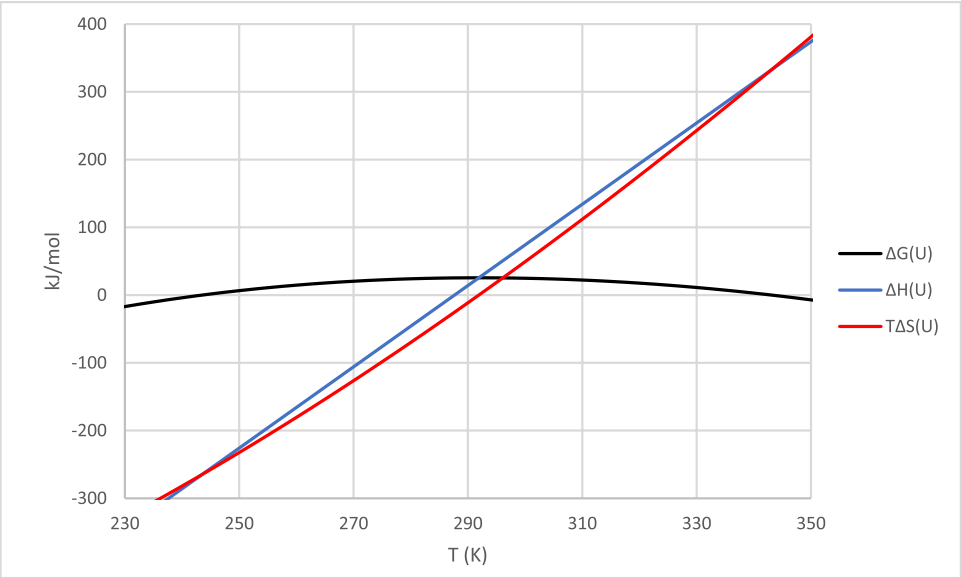

Fig. 5 Stability curve for bovine cytochrome b_5 Data from ref. [93]

(Eq. 18) we know that the energy penalty for burying an unpaired polar or charged group in the low dielectric interior is quite high. For this reason, salt bridges and hydrogen bonds formed in the protein interior are especially strong, and essentially all of the polar and charged groups are paired up in such interactions. This explains why the interior dielectric is so low, even in the presence of so many charged and polar groups.

$$E_{\text{coul}} = \frac{q_1 q_2}{\epsilon r}. \tag{18}$$

One of the key arguments implicating the importance of hydrophobic interactions in stabilizing protein structure is that their stability curves (unfolding free energy change, ΔG°(U), vs. T) resemble those of nonpolar solute o/w transfer (Fig. 2b). For example, the stability curve for bovine cytochrome b_5 is plotted in Fig. 5. This plot resembles the butane plot (Fig. 2), with a few important differences: for the protein, ΔC°_P (the slope of the blue ΔH° vs. T line) is much higher, T_H is slightly lower and T_S is much lower, making ΔT ($= T_S - T_H$) also much lower (i.e., the red $T\Delta S$ curve is closer to the blue ΔH line). These differences and others are compared in Table 5.

The most crucial difference we see from Table 5 is that for the protein unfolding, ΔC°_P is 17 times larger than for butane o/w transfer, because the protein is so much larger (88 amino acid residues, about a third of which are hydrophobic). This increase in ΔC_P drives many of the other differences observed in Table 5. For example, if $\Delta H^\circ(T_{\text{ref}})$ is positive, as it is for protein unfolding at 25 °C (Table 5), then we know from Eq. (5) that increased ΔC_P causes a decline in T_H. Higher ΔC_P causes an even more pronounced decline in T_S, because of the presence of ΔC_P in the exponent (Eq. 7). For example, for neat transfer of small nonpolar solutes (e.g., butane), $T_S \geq 50$ °C, whereas for the unfolding of most proteins (e.g., cytochrome b_5), $T_S \approx 20$–25 °C. The 17-fold higher ΔC_P, together with the lowering of ΔT by fivefold, leaves $\Delta G_{\max}$ about threefold higher (Eq. 10) for cytochrome b_5 unfolding. Perhaps the biggest difference between the two curves is that the two temperature axis intercepts, $T_{G,\text{lo}}$ and $T_{G,\text{hi}}$ are much closer together for the protein ($343 - 244 = 99$ K) than for butane ($448 - 211 = 237$ K). This difference stems from the lower values of T_H and T_S (Eq. 9), which in turn is due to the higher ΔC°_P.

In order to illustrate the effect of ΔC°_P on the stability curve, we plot in Fig. 6 two intermediate curves with values of ΔC°_P, ΔH°_{298}, and ΔS°_{298} that are in between the

Table 5 Comparison of key thermodynamic parameters for *n*-butane neat transfer into water and unfolding of the globular cytochrome b_5 protein, along with two simulated thermodynamically intermediate processes, 1 and 2

	n-Butane (neat transfer)	Cytochrome b_5 (unfolding)	Curve 1	Curve 2
ΔC°_P (kJ/K/mol)	0.35	6.0	2	4
$\Delta G_{\max}$ (at T_S) (kJ/mol)	7.5	25	22	20
T_S (K)	321	292	295	293
T_H (K)	300	288	288	288
$T_{G,\text{lo}}$ (K)	211	244	235	243
$T_{G,\text{hi}}$ (K)	448	343	358	346
ΔH°_{298} (kJ/mol)	− 0.6	63	20	40
$298{\cdot}\Delta S^\circ_{298}$ (kJ/mol)	− 8	38	7	22

For butane and cytochrome b_5, ΔC°_P, ΔH°_{298}, and $298{\cdot}\Delta S^\circ_{298}$ are experimentally determined values. The remainder of the parameters in the table were calculated using Eqs. (5), (7), (9), and (10)

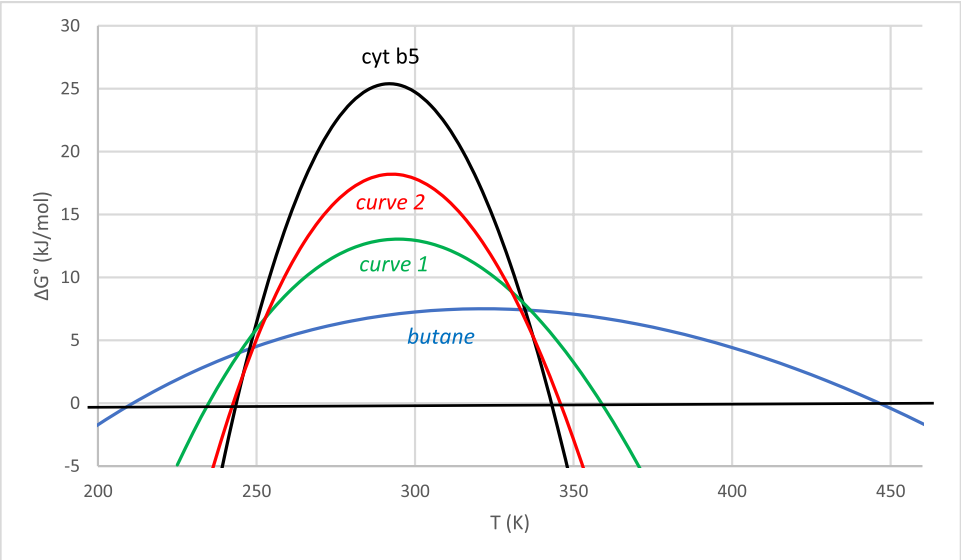

Fig. 6 Stability curves for *n*-butane neat transfer, cytochrome b_5 unfolding, and two thermodynamically intermediate processes. Thermodynamic parameters for the last two processes (curves 1 and 2) can be found in Table 5

low values for *n*-butane neat transfer and the high values for cytochrome b_5 unfolding (Table 5). Note that T_S (the temperature at which ΔG° reaches its maximum value, ΔG°_{max}) decreases by 26 K going from butane to curve 1, and then remains essentially the same for curve 2 and cytochrome b_5; ΔG°_{max} increases steadily from butane to curve 1, 2, and cytochrome b_5. Another big difference is the progressive decrease in $T_{G,hi}$ and increase in $T_{G,lo}$ from butane to curve 1, 2 and cytochrome b_5; thus, ΔT decreases steadily as well.

The significance of the two temperature axis intercepts, $T_{G,lo}$ and $T_{G,hi}$, is that below $T_{G,lo}$ and above $T_{G,hi}$, nonpolar solutes are soluble in water and proteins unfold spontaneously. Proteins therefore undergo both cold and hot denaturation. The former is difficult to observe because it generally occurs at temperatures below the freezing point of water. The latter is referred to as thermal denaturation; $T_{G,hi}$, the high temperature at which the unfolded and folded forms of the protein are in a 50/50 equilibrium, is sometimes referred to as the denaturation temperature (T_{den} or T_d), or alternatively the melting temperature (T_m), even though proteins most decidedly do not "melt"!

Before we go further, it is worth pointing out that another difference between nonpolar solute o/w transfer and protein unfolding is in the sign of ΔH° and ΔS° at room temperature: negative for o/w transfer and positive for unfolding (Table 5). At first glance, this might seem like evidence against the importance of a classical hydrophobic interaction in protein stabilization, but closer consideration shows that this sign difference is simply due to the shift in T_H and T_S. These two values are above room temperature for o/w transfer (Table 5) so ΔH°_{298} and ΔS°_{298} are both negative; for protein unfolding, T_H and T_S are slightly below room temperature so ΔH°_{298} and ΔS°_{298} are both positive. Again, this difference can be traced (at least partly) to the difference in ΔC_P°. Also contributing are, in the folded protein: hydrogen bonding, which raises ΔH°(U); and the low conformational entropy, which raises ΔS°(U). For example, S(folded protein) < S(neat nonpolar liquid) because the nonpolar protein interior is packed tightly, whereas S(unfolded protein) > S(np(aq)) because the long protein chain has so many more degrees of freedom. These two effects combine to make ΔS°_{298}(U) slightly positive.

We have seen that the key factor explaining the negative entropy and nonspontaneity of hydrophobic hydration and o/w transfer is solvent-excluded volume (Eqs. 13, 15, and Appendix). Given the importance of excluded volume, and considering that the van der Waals molar volumes of folded and unfolded proteins are typically about the same [38, 94–97], it seems surprising that the hydrophobic force would figure strongly in protein stabilization. Here is where the importance of shape comes into play [23], along with the difference between van der Waals (hard shell) volume and solvent-excluded volume [38]. Packing is tight and maximally efficient in a protein's native conformation, whereas it is looser in unfolded forms. As a first approximation, native globular proteins can be modeled as efficiently packed spheres, and unfolded forms as more loosely packed spherocylinders (cylinders capped at either end by half-spheres) [38, 95, 96]. Considering a sphere and a spherocylinder of equal volume, it can be shown that the sphere has a significantly smaller solvent-excluded volume and WASA. The extra excluded volume (and WASA) of the unfolded spherocylindrical form explains why the hydrophobic force favors the folded form.

Let us now consider how the unfolding parameters ΔH°_{298}(U), ΔS°_{298}(U), and ΔC°_P(U) affect the protein stability curve. Clearly, ΔG°(U) and stability will increase for proteins with higher ΔH°_{298} and lower ΔS°_{298}; less obvious

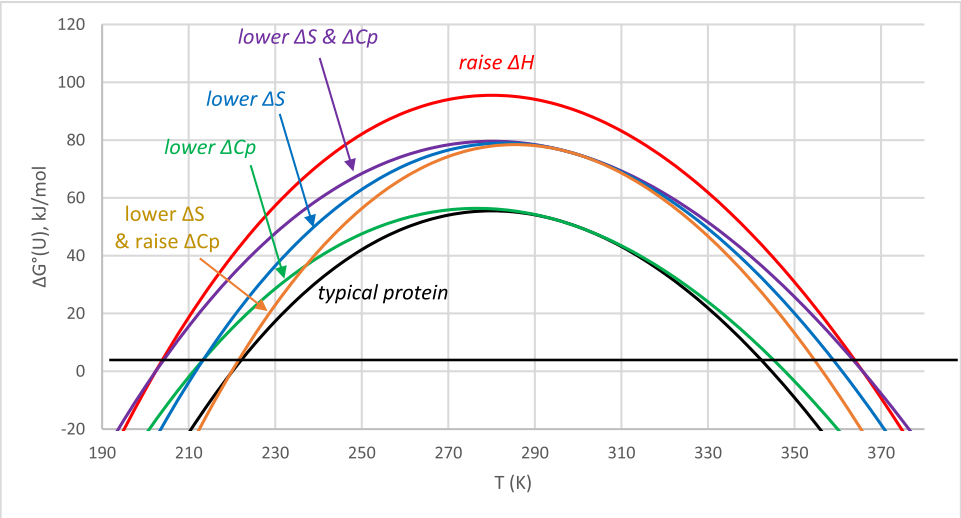

Fig. 7 Protein stability increased over that of a typical protein (black curve) by increasing ΔH°_{298} (red curve), decreasing ΔS°_{298} (blue curve), decreasing ΔC°_P (green curve), decreasing both ΔS°_{298} and ΔC°_P (purple curve), and decreasing ΔS°_{298}/increasing ΔC°_P (gold curve). All changes are by 20%; unfolding thermodynamic parameters are tabulated in the Appendix, Table 8

is that stability rises slightly for proteins with lower ΔC°_P (Fig. 7, green curve). Keep in mind that a stronger hydrophobic effect would be expected to lower ΔS°_{298}(U), but at the same time raise ΔC°_P. These two effects could cancel each other out, but Fig. 7 shows that this is not in fact the case: Lowering ΔS by 20% while raising ΔC_P by the same amount (gold curve) stretches the curve to the right compared to the "typical" protein (black curve): The gold curve has a higher $T_{G,\mathrm{hi}}$, the same $T_{G,\mathrm{lo}}$, and a 40% higher $\Delta G^\circ_{\max}$ (similar to the blue curve, in which ΔS alone is lowered).

Figure 7 also plots how the protein stability curve changes with a 20% rise in ΔH°_{298}(U), and a 20% decline in ΔS°_{298}(U) and/or ΔC°_P(U). All of the changes stretch the stability curve in both directions on the temperature axis, lowering $T_{G,\mathrm{lo}}$ while raising $T_{G,\mathrm{hi}}$. Raising ΔH°_{298} (red curve) is the most effective, stretching the curve by 36 K and increasing $\Delta G^\circ_{\max}$ by over 70%. Lowering ΔC_P (green curve) is the least effective, stretching the curve by 16 K while leaving $\Delta G^\circ_{\max}$ almost unchanged. Lowering ΔS°_{298} (blue, purple, and gold curves) is intermediate.

Two key parameters that can characterize the stability of a folded protein are $T_{G,\mathrm{hi}}$, and $\Delta G^\circ_{\max}$(U), the unfolding free energy at T_S. The former depends on T_H and T_S (Eq. 9), and the latter depends on those two parameters and ΔC°_P(U) as well (Eq. 10). Because thermophiles thrive at high ambient temperatures (up to 120 °C at some undersea thermal vents!), their proteins must have especially high $T_{G,\mathrm{hi}}$ values. However for mesophiles, increasing $T_{G,\mathrm{hi}}$ will not necessarily add stability at intermediate temperatures if $\Delta G^\circ_{\max}$(U) remains unchanged (or even decreases). In other words, to increase the stability of mesophilic proteins at intermediate temperatures, $T_{G,\mathrm{hi}}$ can remain the same as long as $\Delta G^\circ_{\max}$(U) increases. Thermodynamically, this can be accomplished by increasing ΔH°_{298}, ΔS°_{298}, and ΔC°_P, all by the same factor, so that T_H and T_S remain unchanged (Fig. 7, red curve vs. purple curve). Note that the red curve protein is more stable than the purple curve over the entire temperature range from $T_{G,\mathrm{lo}}$ to $T_{G,\mathrm{hi}}$.

On the contrary, thermophilic proteins must be stable at elevated temperatures (above, say, 70 °C) at which mesophilic proteins would spontaneously unfold. There are many combinations of changes in unfolding thermodynamic parameters that yield the required increase in $T_{G,\mathrm{hi}}$. Most of these changes also decrease $T_{G,\mathrm{lo}}$, stretching the stability curve in both directions on the T-axis (Fig. 7).

Thermophilic proteins do not necessarily have to have a lower $T_{G,\mathrm{lo}}$ nor a higher $\Delta G^\circ_{\max}$(U) than mesophilic ones. Lowering all three parameters (ΔH°_{298}, ΔS°_{298}, and ΔC°_P) stretches the curve while lowering $\Delta G^\circ_{\max}$ below the control value (Fig. 8, purple curve); in this case, the protein is stabilized at high and low temperatures, but destabilized at intermediate temperatures. Additionally, there are two ways to raise $T_{G,\mathrm{hi}}$ without lowering $T_{G,\mathrm{lo}}$, i.e., stretching the stability curve to the right (higher temperatures), but not to the left: lowering both ΔH°_{298}(U) and ΔS°_{298}(U), or lowering ΔS°_{298}(U) while raising ΔC°_P(U). In the former case (Fig. 8, blue curve), $T_{G,\mathrm{hi}}$ and $T_{G,\mathrm{lo}}$ both increase, while $\Delta G^\circ_{\max}$ is almost unchanged. In the latter case (red curve), $T_{G,\mathrm{lo}}$ remains unchanged and $\Delta G^\circ_{\max}$ increases as $T_{G,\mathrm{hi}}$ shifts higher.

Figures 7 and 8 depict how the protein stability curve changes when ΔH°_{298}, ΔS°_{298}, and/or ΔC°_P are altered in defined ways. When a mesophilic organism evolves to survive in a high temperature environment, it does so by altering amino acids in its proteins. There are of course many mutational changes in a protein that can alter ΔH°_{298}, ΔS°_{298}, and/or ΔC°_P; furthermore, a single amino acid change can alter one, two, all three, or none of these parameters! It is therefore not surprising that, even though the mathematical relationship between T_H, T_S, $\Delta G^\circ_{\max}$, $T_{G,\mathrm{hi}}$, and ΔC°_P is

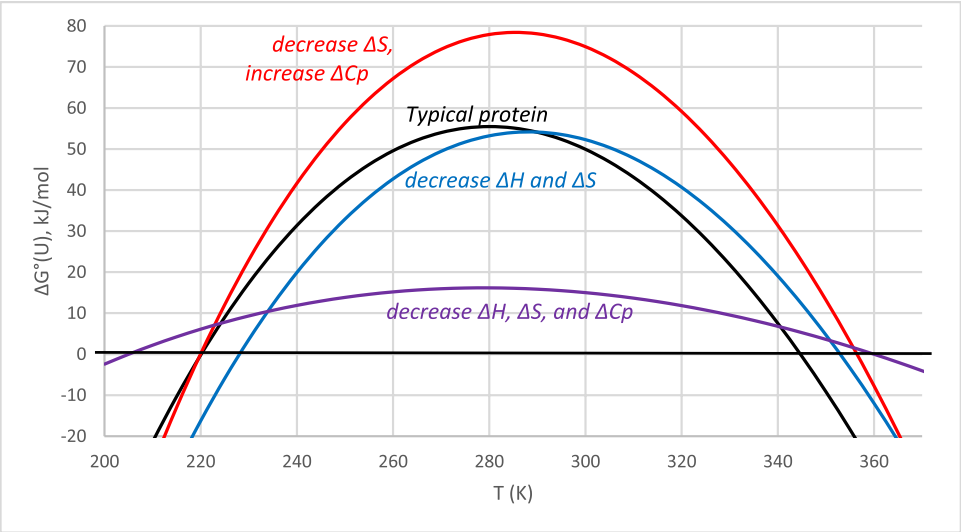

Fig. 8 Unusual thermophilic stability curves. Lowering all three parameters (ΔH°_{298}, ΔS°_{298}, and ΔC_P°) stretches the curve while lowering ΔG°_{max} below the typical value (purple curve). $T_{G,hi}$ is raised by decreasing both ΔS°_{298} and ΔH_{298}° (blue curve), or by decreasing ΔS°_{298} and increasing ΔC_P° (red curve). Unfolding thermodynamic parameters are tabulated in the Appendix, Table 8

Table 6 Unfolding thermodynamic parameters for mesophilic, thermophilic, and thermophobic proteins

	Thermophobic[a]	Mesophilic[b]	Thermophilic[c]
ΔC°_P(U) (J/K/mol AA)[d]	62 ± 3	61 ± 17	56 ± 28
ΔH°_{298}(U) (kJ/mol AA)[d]	1.33 ± 0.22	1.1 ± 0.8	0.3 ± 0.9*
$298{\cdot}\Delta S^\circ_{298}$(U) (kJ/mol AA)[d]	1.31 ± 0.18	0.9 ± 0.7	−0.2 ± 0.9*
ΔG°_{max}(U) (kJ/mol AA)[d]	0.07 ± 0.05**	0.26 ± 0.13	0.5 ± 0.3*
T_S (K)	277.(6) ± 3	283 ± 13	299 ± 16*
T_H (K)	276.(4) ± 4	278 ± 16	289 ± 20*
ΔT (K)	1.2 ± 0.9**	5 ± 3	9.(3) ± 6*

*Difference (thermophilic vs. mesophilic) is statistically significant: P value < 0.003

**Difference (mesophilic vs. thermophobic) is statistically significant: P value < 0.015

[a]For thermophobes, $T_{G,hi} \leq 36$ °C; $n = 5$ proteins; data from [93].

[b]For mesophiles, 36 °C < $T_{G,hi} \leq 82$ °C; $n = 83$ proteins; data from refs. [93, 99–101]

[c]For thermophiles, $T_{G,hi} > 82$ °C; $n = 38$ proteins; data from refs. [93, 99–102]

[d]Because hydrophobicity thermodynamic parameters scale with the number of nonpolar groups in the molecule, in order to normalize the values for the purposes of comparison, they are divided by the number of amino acid residues in each protein

straightforward (Eqs. 5, 7, 9, 10), when comparing different proteins, no obvious correlation is found between these parameters [98]. There are simply too many ways that these thermodynamic parameters can change when amino acids are altered. Nevertheless, by comparing the stability curves of mesophilic, thermophilic, and thermophobic proteins, some conclusions can be drawn (Table 6).

Firstly, the average ΔC°_P (U, per amino acid) is statistically the same for all three types of proteins; this matches the conclusion of Graziano [98]. Because increasing the strength of the hydrophobic force must raise ΔC_P, this suggests that at least on average (see below), adaptation toward thermotolerance does not proceed by increasing hydrophobicity.

Secondly, average values of both ΔH°_{298} and ΔS°_{298} are lower for thermophilic proteins compared to mesophilic ones. Thirdly, ΔG°_{max}, T_S, T_H, and ΔT ($= T_S - T_H$) are all higher for thermophilic proteins compared to mesophilic ones. This suggests that the stability curve for the average thermophilic protein is both higher and broader than the average mesophilic stability curve (Fig. 9). Finally, comparing mesophilic and thermophobic proteins, the only statistically significant differences are for ΔG°_{max} and ΔT, both of which are higher for mesophilic proteins. Stability curves for the three types of proteins, using the average thermodynamic unfolding parameters in Table 6, are depicted in Fig. 9. Thermophobic proteins (blue curve) are clearly the least stable, both in terms of their low ΔG°_{max}(U), and the narrow temperature range over which the protein remains folded (i.e., ΔG°(U) is positive): Not only do these proteins thermally denature at relatively low temperatures (> 30 °C), they also cold denature at relatively high temperatures (< − 20 °C).

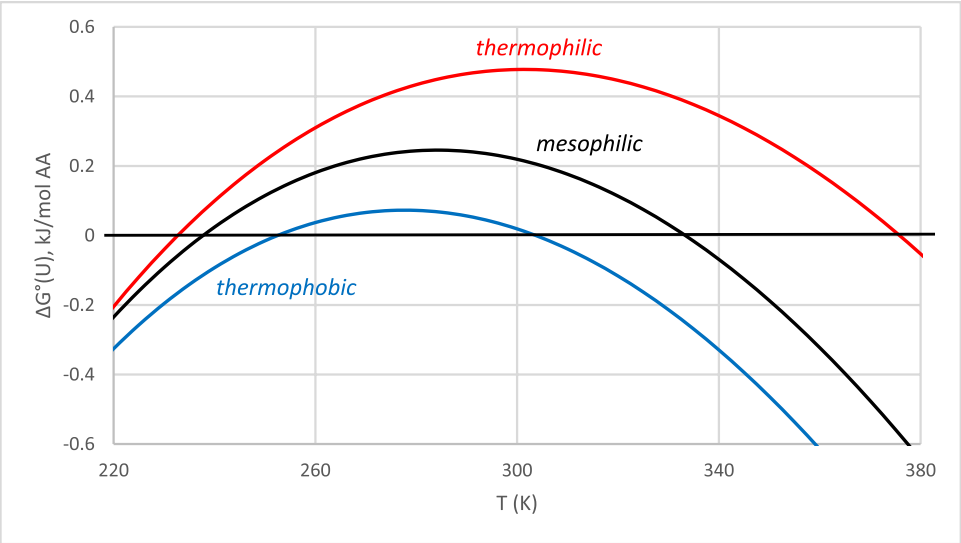

Fig. 9 Stability curves for thermophobic (blue curve), mesophilic (black curve) and thermophilic (red curve) proteins, using the average thermodynamic unfolding parameters in Table 6

It is interesting that ΔS°_{298} for the average thermophilic protein is not only less than that for a mesophilic protein, it is in fact essentially zero (Table 6). This has been interpreted as being due to residual structure that remains in the unfolded forms of thermophilic proteins; this structure in the U form lowers its entropy, and decreases ΔS(U). Restricted flexibility in unfolded thermophilic proteins stems from having more salt bridges and prolines, shorter loops, and replacement of arginine with lysine [94, 99].

A good way to examine more closely how the evolutionary process alters protein stability thermodynamic parameters is to examine sets of homologous proteins [94, 98–100]. The advantages are that homologous proteins are often roughly the same size and shape, and the number of amino acid differences is fairly low. This gives us a better chance at discerning trends in how changes in the stability curve and in the unfolding thermodynamic parameters accompany evolution from mesophilic to thermophilic (or psychrophilic, cold-loving) organisms.

Before we examine how nature solved the problem of mesophilic to thermophilic adaptation, it is a good idea to summarize the options laid out in Figs. 7, 8, 9 and Table 6. Protein stability is enhanced by a rise in ΔH°_{298}(U), a decline in ΔS°_{298}(U), a decline in ΔC°_P(U), or various combinations of these changes. Protein stability curves can change in five ways:

(I) By far the most common is for the curve to stretch both right and left, as $T_{G,\mathrm{hi}}$ increases and $T_{G,\mathrm{lo}}$ decreases. $\Delta G^\circ_{\max}$ and T_S can increase, decrease, or remain the same.

(II) The curve shifts to the right: both $T_{G,\mathrm{hi}}$ and $T_{G,\mathrm{lo}}$ increase. T_S must increase, and $\Delta G^\circ_{\max}$ can increase or remain the same.

(III) The curve stretches to the right: $T_{G,\mathrm{hi}}$ increases and $T_{G,\mathrm{lo}}$ remains the same. T_S must increase, and $\Delta G^\circ_{\max}$ generally increases.

(IV) The curve stretches to the left: $T_{G,\mathrm{lo}}$ decreases and $T_{G,\mathrm{hi}}$ remains the same. T_S must decrease, and $\Delta G^\circ_{\max}$ can increase or remain the same. This is a psychrophilic adaptation.

(V) The curve increases in height only: $T_{G,\mathrm{lo}}$ and $T_{G,\mathrm{hi}}$ remain the same, as does T_S; $\Delta G^\circ_{\max}$ increases. This is the rarest change.

In light of the five types of stability curve shifts summarized above, our next question is, what has Nature done? As an example, Fig. 10 shows stability curves for five homologous cold shock proteins. Bc-CspB has the lowest $T_{G,\mathrm{hi}}$ (black curve), so it is considered the "typical" mesophilic form. The four other curves represent curve shift types I (blue), II (red), III (gold), and V (purple). Examples of type IV are found in SH3 proteins (not shown), but not in cold shock proteins. Note that for the cold shock proteins, $\Delta G^\circ_{\max}$ increases for all four thermophiles; T_S increases for types II and III, but it decreases slightly for type I.

Table 7 lists comparative results for 36 homologous protein pairs (39 pairs for T_S and 43 pairs for $\Delta G^\circ_{\max}$). We see that $T_{G,\mathrm{lo}}$ declines in most pairs, so type I is the most common shift; furthermore, $\Delta G^\circ_{\max}$ increases in the overwhelming majority of pairs (86%). T_S increases in almost half of all pairs, but a lower or unchanged T_S is not uncommon. Decreasing ΔS°_{298} is about twice as common as increasing (64% vs. 30%), whereas for ΔH°_{298}, increasing and decreasing are about equally common (50% vs. 42%). ΔC°_P is split almost evenly between increasing, decreasing, and remaining the same; this matches the averaged results from Table 6. All 10 of the pairs (28%) that featured an increase in ΔC°_P

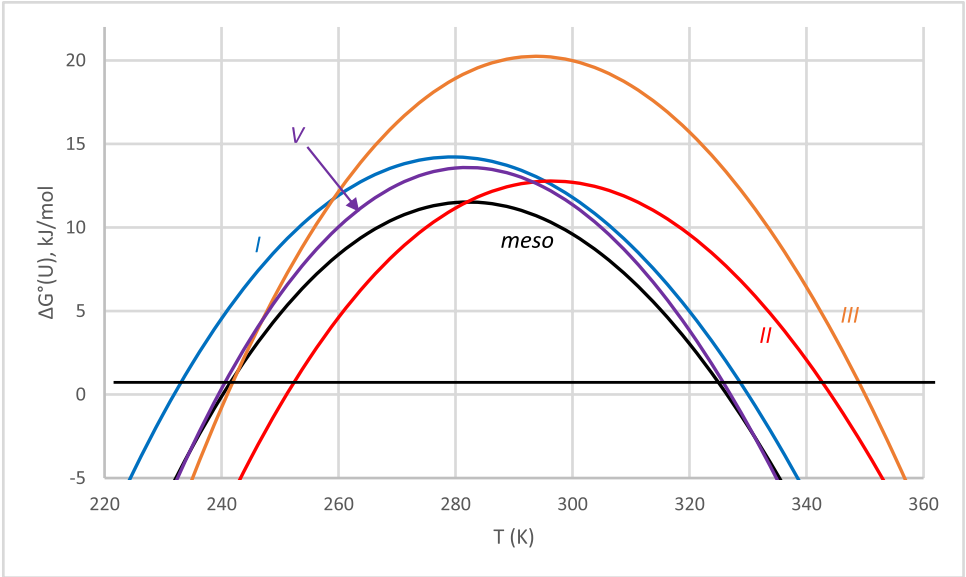

Fig. 10 Stability curves for five cold shock proteins. The "typical" mesophilic protein is Bc-CspB (black curve); the type I curve is EC-CspA (blue curve); type II = TB-CspB (red curve); type III = Bc-Csp (gold curve); and type V = Bs-CspB (purple curve) Data from ref. [94]

Table 7 Unfolding thermodynamic parameters for homologous pairs of proteins in which $T_{G,hi}$ either increased or remained the same

Parameter	Increase (%)[a]	Decrease (%)[a]	Unchanged (%)	# pairs
$T_{G,hi}$	89	0	11[b]	36
$T_{G,lo}$	17	69	14	36
T_S	46	18	36	39
$\Delta G^\circ_{max}(U)$	86	5	9	43
ΔC°_P	28	39	33	36
$\Delta H^\circ_{298}(U)$	42	50	8	36
$\Delta S^\circ_{298}(U)$	30	64	6	36

Homologous sets include: SH3 proteins ($n=11$), Sac/Sso ($n=7$), cold shock proteins ($n=7$), histidine-phosphate carrier proteins (HPr, $n=5$), histone proteins (MfB, $n=4$), lysozyme T4 ($n=22$), isopropyl malate dehydrogenase ($n=2$), DNA methyl transferase ($n=2$), CheY ($n=2$), ribosomal L30E ($n=2$), DNA binding domains ($n=2$), and RNAase H ($n=2$). Data are from Razvi and Scholz (15 pairs, [100]), Pica and Graziano (21 pairs, [94]), Rees and Robertson (3 pairs, [93]), and Robertson and Murphy (4 pairs, [102])

[a]For each set of homologous proteins, the one with the lowest $T_{G,hi}$ was deemed the "typical" or mesophilic one, and differences of others in the set were considered relative to this protein. For the four pairs in which $T_{G,hi}$ was the same, the protein with the highest $T_{G,lo}$ was deemed the "typical" or mesophilic one

[b]These four were mesophilic/psychrophilic pairs

also showed a decrease in ΔS°_{298}, probably a sign of increasing hydrophobic force stabilizing the thermophilic protein.

Based on our expectation of enthalpy–entropy compensation, it is not surprising that 80% of the pairs have ΔS°_{298} and ΔH°_{298} moving in the same direction: both parameters decreased in 50% of pairs, and both increased in 30% of pairs. Of the seven remaining pairs, one had no change in either parameter, one had ΔS°_{298} unchanged (and ΔH°_{298} rising), two had ΔH°_{298} unchanged (and ΔS°_{298} falling), and surprisingly, three pairs had ΔS°_{298} falling and ΔH°_{298} rising. Clearly enthalpy–entropy compensation is skirted by these three protein pairs.

Finally, in terms of the five types of stability curve changes summarized above, just over half were type I, almost 20% were type II, 11% type III, 14% type IV, and only one pair (3%) was type V. Interestingly, for the type II and III pairs, the thermophilic protein showed an increase in $\Delta C^\circ_P(U)$ and a decrease in $\Delta S^\circ_{298}(U)$, which is the hallmark of a stronger hydrophobic force. On the other hand, a number of reports point to the importance of increased salt bridging in the stabilization of thermophilic proteins [94, 99]. This should result in a decrease in $\Delta C^\circ_P(U)$ and an increase in $\Delta H^\circ_{298}(U)$ and $\Delta S^\circ_{298}(U)$, which is observed in 30% of the pairs in Table 7. The remaining 40% of pairs did not show a simple hydrophobic or salt bridge thermodynamic signature. The take-home lesson here is that Nature has many pathways to evolve thermostability, and She does not seem to have a preference for any single one: increased hydrophobicity and salt bridging are important in about 60% of the pairs examined, but the remaining evolutionary paths led to less "correlated" changes in $\Delta C^\circ_P(U)$, $\Delta H^\circ_{298}(U)$, and $\Delta S^\circ_{298}(U)$ that still managed to increase thermostability.

Binding: classical vs. nonclassical hydrophobic effect

The driving force for proteins binding to ligands, substrates, or other proteins is a combination of the same forces that stabilize protein folding. Charged ligands can utilize salt bridging, polar ligands can utilize hydrogen bonding, and nonpolar ligands can utilize the hydrophobic force (amphiphilic ligands can utilize a combination of these interactions). Quite a few important

agonists, antagonists, and drugs are nonpolar, so the hydrophobic effect on receptor and enzyme function is expected to be significant. Binding to exposed hydrophobic patches on misfolded proteins has been implicated in the heat shock response, protein damage scavenging, and the innate immune response [103].

By examining the thermodynamics of ligand binding, one should be able to tease out the significance of the hydrophobic effect. Recall that the binding of a nonpolar ligand to a hydrophobic binding site (Table 2, reaction iii) should resemble a hydrophobic interaction (HI: nonpolar phase segregation/aggregation), the reverse of hydrophobic neat transfer. For HI/binding the enthalpy and entropy, $\Delta H^{\circ}_{b,HI}$ and $\Delta S^{\circ}_{b,HI}$, should both be positive, and $\Delta C^{\circ}_{P,HI}$ should be negative. Such a hydrophobic thermodynamic signature is indeed observed for some nonpolar ligands [104–106], but not for others [104, 106–109]. Binding of the latter ligands, featuring ΔH°_{b}, ΔS°_{b}, and $\Delta C^{\circ}_{P,b}$ that are all negative, has been dubbed a "nonclassical" hydrophobic effect.

Since Ross and Subramanian's 1981 paper [107], a body of literature has grown up interpreting this nonclassical hydrophobic effect as being due to suboptimal, disordered hydration of the receptor's hydrophobic binding pocket [108, 110, 111]. Although this may in fact be the case, it is important to point out that this same thermodynamic signature is seen in protein unfolding, and it is expected if the reference temperature happens to be above T_S. As is the case for protein unfolding, this reversal of the expected sign for ΔH and ΔS does not necessarily mean that the "classical" hydrophobic effect does not apply, it just means that the reference temperature is high and/or T_S is lower than is typically observed for nonpolar solute hydration. This is not surprising because most of the ligands studied are not purely hydrophobic, but rather amphiphilic, as are the binding sites on the protein receptor. Thus, it seems quite reasonable that some of these binding interactions have a thermodynamic signature resembling protein folding rather than nonpolar solute hydration.

Conclusions

Since the 1998 publication of my first pedagogical review of the hydrophobic effect, four major new conclusions have arisen in the literature:

1. The thermodynamics of the hydrophobic effect are controlled mainly by the nonpolar solute–water intermolecular forces (ΔH°_{IMF}) and solute cavity solvent-excluded volume ($\Delta S^{\circ}_{excl.vol.}$). Both of these increase in magnitude with solute size, which explains the well-known size-dependence of the hydrophobic effect thermodynamic parameters.
2. The "iceberg" model is not well supported. Although there is good evidence for the existence of some increased order and H-bond stability in the hydration shell, this is not enough to explain the large positive ΔC_P and the large negative room-temperature ΔS. These are best explained by solvent-excluded volume and properties of pure water: its equation of state, thermal pressure coefficient, strong cohesive forces, and small size (enhanced excluded volume effect).
3. A "nonclassical" hydrophobic effect (positive ΔH and ΔS at room temperature, positive ΔC_P) has been invoked for the hydration of large solutes (> 10 Å radius) and the binding of some ligands. Calorimetric studies have not borne out this "nonclassical" effect for various large nonpolar solutes, including long-chain carboxylic acids, polymers, fullerenes, graphenes, and portions of protein surfaces. Interestingly, although protein unfolding displays the same positive signs of ΔH, ΔS, and ΔC_P, no one has ever referred to protein unfolding as a "nonclassical" hydrophobic effect. For both protein unfolding and ligand binding, the room temperature positive values of ΔH and ΔS occur simply because T_H and T_S, respectively, are below 25 °C. This, in turn, is true because the water-exposed groups are amphiphilic, including a significant number of polar groups.
4. Protein stability can be enhanced in a number of ways, the most common being increasing the room temperature unfolding enthalpy ($\Delta H^{\circ}_{298}(U)$), decreasing $\Delta S^{\circ}_{298}(U)$, and/or decreasing $\Delta C^{\circ}_{P}(U)$. Changes in unfolding thermodynamic parameters suggest that enhancing the hydrophobic effect and the number and strength of salt bridges has occurred in more than half of thermophilic proteins. For the remainder, presumably, stability has been increased by a combination of these two effects, along with increased hydrogen bonding and disulfide bridging.

Acknowledgements I wish to express profound gratitude to Giuseppe Graziano and Henry Ashbaugh, both of whom have helped me to grapple with the recent literature, and patiently answered my many questions. Bob Gennis also read over the first draft and gave me some cogent editing suggestions.

Appendix

Enthalpy, entropy convergence for hydrophobic hydration

In his massive and influential 1979 review of protein stability [112], one of the observations that Privalov made was that at about 100–110 °C, compact globular proteins

Table 8 Unfolding thermodynamic parameters for curves plotted in Figs. 7 and 8

	ΔC°_P(U) (kJ/K/mol)	ΔH°_{298}(U) (kJ/mol)	ΔS°_{298}(U) (kJ/mol/K)	T_S (K)	T_H (K)	ΔG°_{max}(U) (kJ/mol)
Typical	8.0	200	0.5	280.1	273.2	55.5
Figure 7, blue	8.0	200	0.4 *(20% decr.)*	283.0	273.2	79.0
Figure 7, red	8.0	240 *(20% incr.)*	0.5	280.1	268.2	95.5
Figure 7, green	6.4 *(20% decr.)*	200	0.5	276.6	268.2	56.4
Figure 7, purple	6.4 *(20% decr.)*	200	0.4 *(20% decr.)*	280.1	268.2	79.6
Figure 8, red	9.6 *(20% incr.)*	200	0.4 *(20% decr.)*	285.5	277.3	78.4
Figure 8, blue	8.0	133 *(33% decr.)*	0.27 *(46% decr.)*	288.3	281.5	54.2
Figure 8, purple	1.5 *(81% decr.)*	45 *(77% decr.)*	0.1 *(80% decr.)*	278.9	268.2	16.2

% changes from the "typical" value are given in parentheses

converged on the same value of specific enthalpy of unfolding (cal/g). He found a similar convergence for the specific entropy of unfolding around 110 °C, although the effect was not nearly as clear.

In 1986, Robert Baldwin published a keystone paper [116] in which he compared the thermodynamics of liquid hydrocarbon neat transfer to the unfolding of the enzyme lysozyme. He found that for six hydrocarbons (benzene, toluene, ethylbenzene, cyclohexane, *n*-pentane, and *n*-hexane), T_H and T_S were approximately the same: $T_H = 22 \pm 5$ °C, and $T_S = 113 \pm 3$ °C.[7] Baldwin then applied these values to the temperature-dependent unfolding of hen lysozyme by splitting protein stability into a hydrophobic effect (HE) and a non-hydrophobic effect (NHE, $\Delta X_{obs} = \Delta X_{HE} + \Delta X_{NHE}$), and assuming that (1) ΔC°_P(U) is entirely due to the HE, and (2) for the effect of hydrophobicity on protein unfolding, T_H and T_S are identical to the liquid hydrocarbon neat transfer values. Using Eqs. (4) and (6) (main text), Baldwin calculated HE ΔH°_{298} and ΔS°_{298}, and then by subtracting from the net observed ΔH°_{298} and ΔS°_{298}, he calculated the NHE values. Both NHE values were temperature-independent: ΔH°_{298}(U, NHE) = +217.8 ± 0.7 kJ/mol, and ΔS°_{298}(U, NHE) = +2294 ± 3 J/K/mol. The former value was interpreted as the cost, upon unfolding, of breaking polar interactions (e.g., H-bonds), and the latter the increase in conformational entropy, i.e., the release of polypeptide chain positioning constraints.

In 1990, Murphy and Gill took this analysis a step further, defining the notion of "convergence" temperatures for enthalpy and entropy [10, 13, 114, 115]. They started by applying Baldwin's HE/NHE breakdown to the temperature dependence of enthalpy, considering a series of homologous compounds (e.g., noble gases, alkanes, alcohols, amines) which shared the same functional group and differed only in their hydrophobicity (e.g., size of noble gas or number of carbons). The hydration enthalpy can then be envisioned as comprising a hydrophobic term that increases with solute hydrophobicity, and a non-hydrophobic term that is independent of hydrophobicity. Enthalpy convergence would then occur at some temperature, $T_{H,conv}$, at which all of the homologous compounds in the series have the same hydration enthalpy, ΔH_{conv}. Thus, at the convergence temperature, ΔH° of hydration depends only on the nature of the series (i.e., the functional group), and not on the individual compound. With this in mind, the temperature dependence of ΔH (main text Eq. 2), can be cast as

$$\begin{aligned}\Delta H^\circ(T) &= \Delta H^\circ(T_{ref}) + \Delta C^\circ_P(T - T_{ref}) \\ &= \Delta H^\circ(T_{H,conv}) + \Delta C^\circ_P(T - T_{H,conv}).\end{aligned} \tag{19}$$

Normally, one would use Eq. (19) along with measured values of ΔH° at various temperatures to determine ΔC°_P. If, however, one already knows ΔC°_P for each compound in the series, then measured values of ΔH° at a specific reference temperature (e.g., 298 K) can be used in the following version of Eq. (19):

$$\Delta H^\circ_{298} = \Delta H^\circ(T_{H,conv}) + \Delta C^\circ_P(298 - T_{H,conv}). \tag{20}$$

Thus, a plot of ΔH°_{298} vs. ΔC°_P for each compound in the series will give a straight line with slope = $(298 - T_{conv})$ and intercept = $\Delta H^\circ(T_{conv})$. This is sometimes referred to as an MPG (Murphy–Privalov–Gill) plot. Because $\Delta H^\circ(T_{conv})$ characterizes the entire series, it must apply to what remains the same in the series, i.e., the non-hydrophobic component of the observed net ΔH°; thus, it would be different for a series of alkanes vs. alcohols vs. amines. On the other hand, T_{conv} should be the same for alkanes, alcohols, and amines because they all differ by the same hydrophobic parameter, i.e., the number of carbons.

[7] It is important to note that Baldwin used the mole fraction = 1 standard state, rather than the more appropriate 1 M standard state recommended by Ben Naim [113]. T_S would be much lower using the molarity standard state.

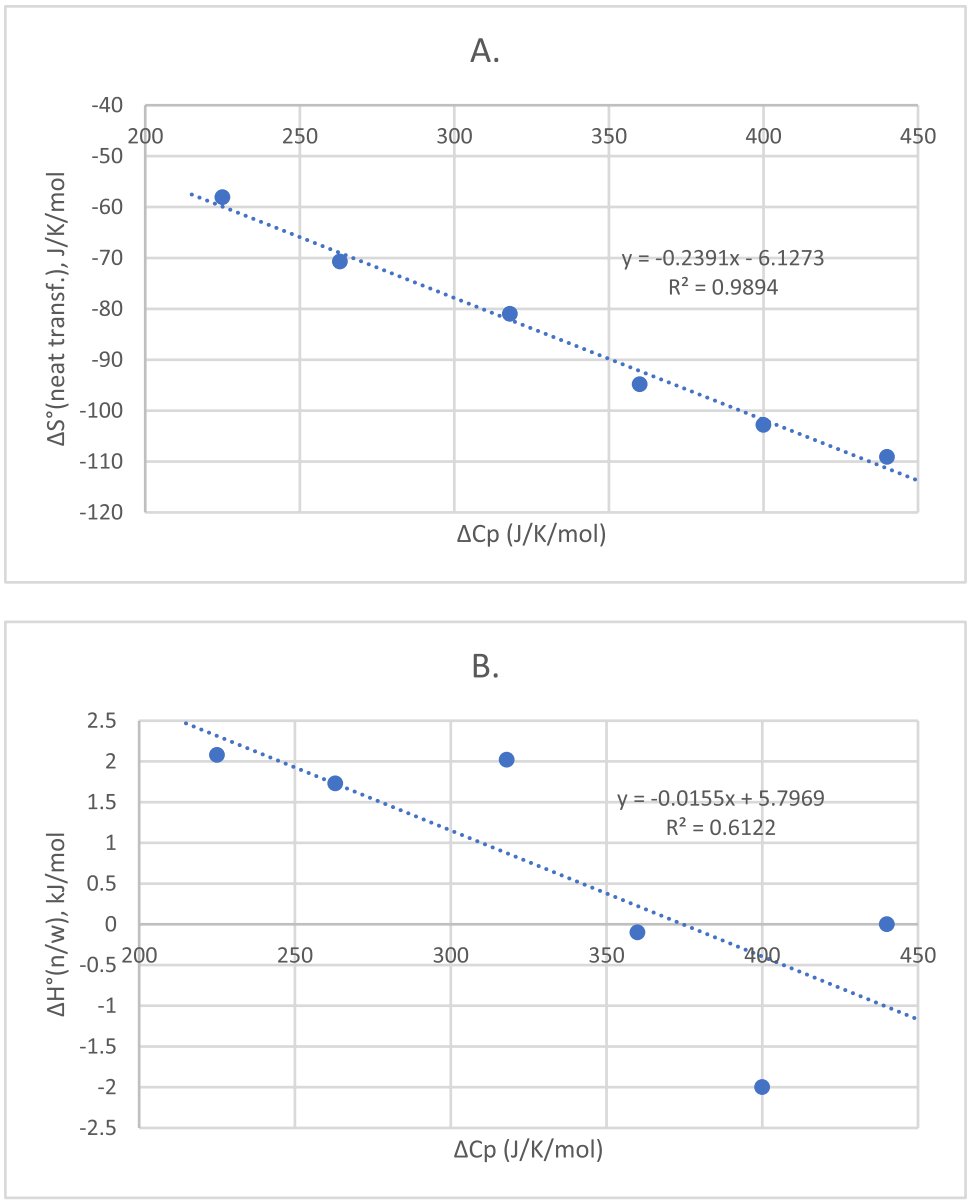

Fig. 11 MPG plots of liquid hydrocarbon neat transfer. **a** Entropy; **b** enthalpy; liquids are benzene, toluene, ethylbenzene, cyclohexane, *n*-pentane, and *n*-hexane Data from ref. [116]

A similar analysis of entropy leads to this adaptation of Eq. (3) in the main text:

$$\Delta S^{\circ}_{298} = \Delta S^{\circ}(T_{S,\mathrm{conv}}) + \Delta C^{\circ}_{P} \cdot \ln(298/T_{S,\mathrm{conv}}). \quad (21)$$

The MPG plot here would be $\Delta S^{\circ}{}_{298}$ vs. $\Delta C^{\circ}{}_{P}$, with slope $= \ln(298/T_{S,\mathrm{conv}})$, and intercept $= \Delta S^{\circ}(T_{S,\mathrm{conv}})$. As with enthalpy, $\Delta S^{\circ}(T_{\mathrm{conv}})$ characterizes the entire series, so it must apply to the non-hydrophobic component of the observed net ΔS°.

For example, MPG plots of Baldwin's liquid hydrocarbon neat transfer data [116] do show a linear correlation (Fig. 11), although the relationship is not very strong for ΔH ($R^2 = 0.6$). From the slopes, the convergence temperatures are calculated to be $T_{S,\mathrm{conv}} = 106 \pm 5$ °C; $T_{H,\mathrm{conv}} = 40 \pm 6$ °C. Note that these temperatures are close to, but not identical to T_S and T_H.

Figure 11a, with its excellent linearity, suggests that entropy convergence for the neat transfer of this series of liquid hydrocarbons does occur. The relative uncertainty in the convergence temperature is good, at only 4% ($= 100 \times 4.7/106$). (For $\Delta S^{\circ}(T_{S,\mathrm{conv}})$, however, it is 70%!) Thus, we might expect to see a fairly robust isosbestic point in the ΔS° vs. T plot for neat transfer (Fig. 12). Sadly, that is not actually the case.

The first thing to note from Fig. 12 is that for all six liquids, T_S, the temperature at which each curve crosses the T-axis, lies between 382 and 390 K; this matches the average

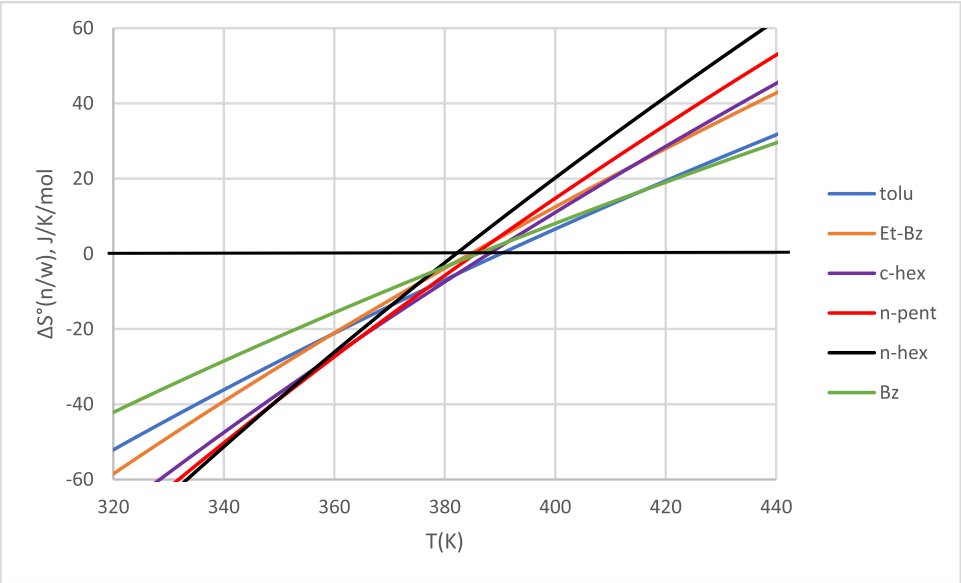

Fig. 12 Temperature dependence of the entropy of neat transfer of liquid hydrocarbons Data from ref. [116]

value reported above (113 ± 3 °C). Most of the curves cross each other (shared values of $\Delta S°$) between about 360 and 390 K; this also matches the calculated convergence temperature from the MPG plot, 106 ± 5 °C. However, there are several intersections below 360 K, and several more above 400 K. The lack of a clear isosbestic point suggests that the entropic convergence behavior is not nearly as robust as one might have expected from the MPG plot. A similar "smeared" isosbestic is observed in the $\Delta H°$ vs. T curve intersections, stretching from 300 to 345 K (data not shown). At least some of this "blurring" of the expected isosbestic point has been shown to be due to the temperature dependence of ΔC_P [117]. Beyond this though, one may question the assumptions in the convergence derivation, namely, that the hydrophobic and non-hydrophobic contributions can be separated out and that the former really are identical for every member of the homologous series of compounds. Graziano [32] and Pratt [117] have supported the existence of entropy convergence for families of small solutes, but rejected enthalpy convergence (Graziano, personal communication).

Murphy, Privalov, and Gill published an extremely influential paper in 1990 in which they compared MPG plots of Baldwin's liquid hydrocarbon data with nonpolar gas hydration, solid → water transfer of nonpolar cyclic peptides, and protein unfolding [10]. They found that the slopes of all four of the $\Delta S°$ vs. $\Delta C°_P$ plots were nearly identical, ranging from − 0.23 ± 0.04 to − 0.28 ± 0.01. Thus $T_{S,\mathrm{conv}}$ for all four of these sets of compounds lie in a fairly narrow range between 102 ± 15 and 121 ± 6 °C; this pointed to the "dominant role that water [and the hydrophobic effect] play in determining the [entropy] of hydration of [all of] these compounds" [10].

Murphy, Privalov, and Gill drew another interesting conclusion from the intercepts of their MPG plots [10]. They determined $\Delta S°(T_{S,\mathrm{conv}})$ to be − 78.5 ± 2.5 J/K/mol for nonpolar gas hydration vs. − 6 ± 4 J/K/mol for liquid neat transfer; this is expected, because gases lose much more freedom of motion upon transfer to the aqueous phase than liquids do. Meanwhile, $\Delta S°(T_{S,\mathrm{conv}})$ was quite similar for protein unfolding (18 ± 1 J/K/mol) and the transfer of solid nonpolar cyclic peptides into water (16 ± 1 J/K/mol). This corroborated previous findings that in terms of packing and freedom of motion, the protein interior is best modeled as a solid organic compound, rather than a liquid [118–120].

To give some idea of the linearity of the MPG plots in the 1990 *Science* paper, Fig. 13 plots the nonpolar gas hydration and protein unfolding results. Note that once again, the linear fits are good ($R^2 = 0.89$ for gas hydration, 0.96 for protein unfolding), and the slopes are fairly close (− 0.068 and − 0.077). In light of how influential the 1990 Murphy, Privalov, and Gill paper was, it is surprising that no one seems to have checked to see whether these gases and proteins actually demonstrated isosbestic behavior in their $\Delta H°$ vs. T plots. In Fig. 14 I have plotted the five members of each series that lie closest to the linear fit line in the MPG plots. As with liquid hydrocarbon neat transfer (Fig. 12), many of the crossings lie in a fairly narrow range of temperature (355–365 K for A and 370–380 K for B), but a number of crossings occur far outside this range.

Perhaps the most interesting part of this story about convergence came to light in the years after 1990, as more protein unfolding thermodynamic data became available. Twelve proteins were originally tabulated in Privalov and Gill's 1988 review [101], 11 of which were included in their 1990 MPG plot [10]. It turned out that not only was the

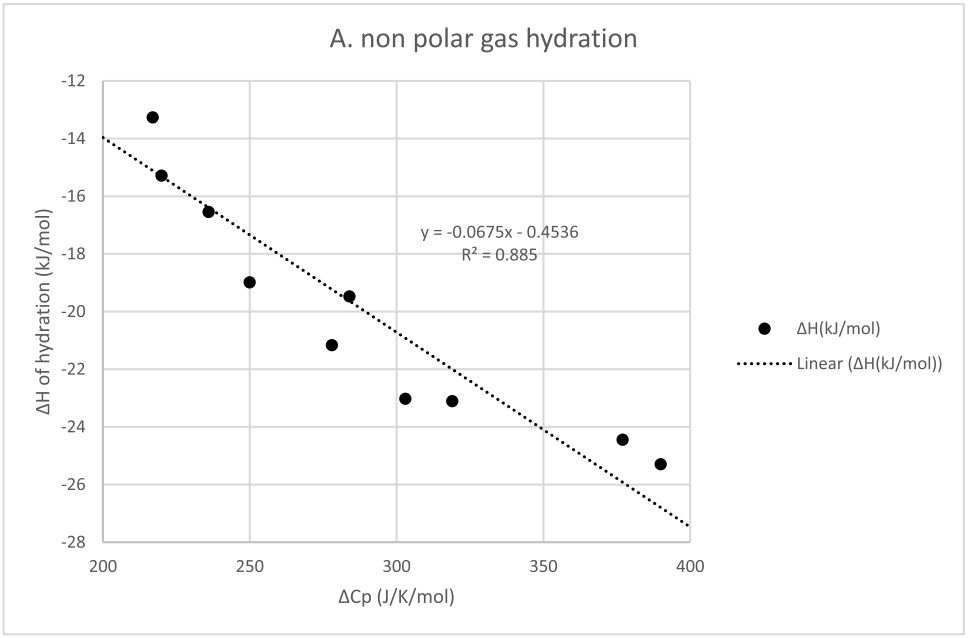

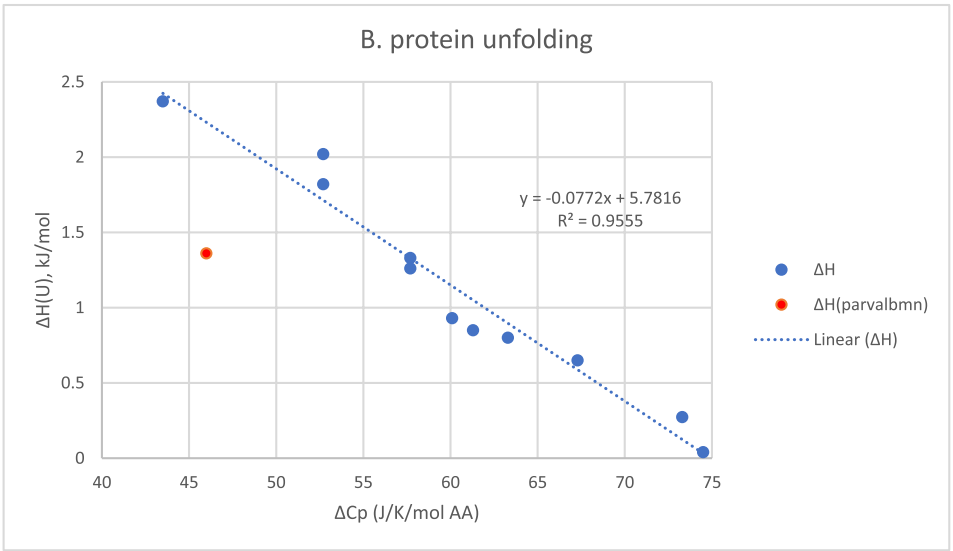

Fig. 13 MPG enthalpy plots of **a** nonpolar gas hydration; and **b** protein unfolding; data from ref. [101]. Without giving any reason, MPG omitted the parvalbumin unfolding data point (red) from their published plot

omitted point (suspiciously?) far off the fit line (Fig. 14b), but the 11 points included were extraordinarily unusual in their linearity.

This was discovered in 1997, when Robertson and Murphy published a review in which they tabulated unfolding thermodynamic data for 65 globular proteins of known structure [102]. The MPG plots in this paper had R^2 values of only 0.36 and 0.33; unsurprisingly, the convergence temperatures calculated from the slopes of these plots (66 °C for enthalpy, 65 °C for entropy) were much different from those in the 1990 paper (102 °C for enthalpy, 106 °C for entropy).[8] Robertson and Murphy's conclusion from these disappointing MPG plots was that the convergence behavior for this much larger set of unfolded proteins was "not very compelling." Huang and Chandler [121], using Lum–Chandler–Weeks theory [18], showed that the convergence temperature should decrease with increasing protein size, thus "one may not expect to observe a convergence temperature for the entropy of unfolding for all proteins." Considering the diversity of protein groups that are exposed to water upon unfolding, as well as the change in shape, it is not surprising that proteins do not behave like a set of homologous compounds all with the same functional group. (And as we have seen, the convergence behavior even in this best of cases is not as clear as one might hope.) This failure

[8] An update of this plot including 100 proteins gave similar results: R^2 values of 0.35 and 0.29; convergence temperatures of 63 °C for enthalpy, 60 °C for entropy (data not shown).

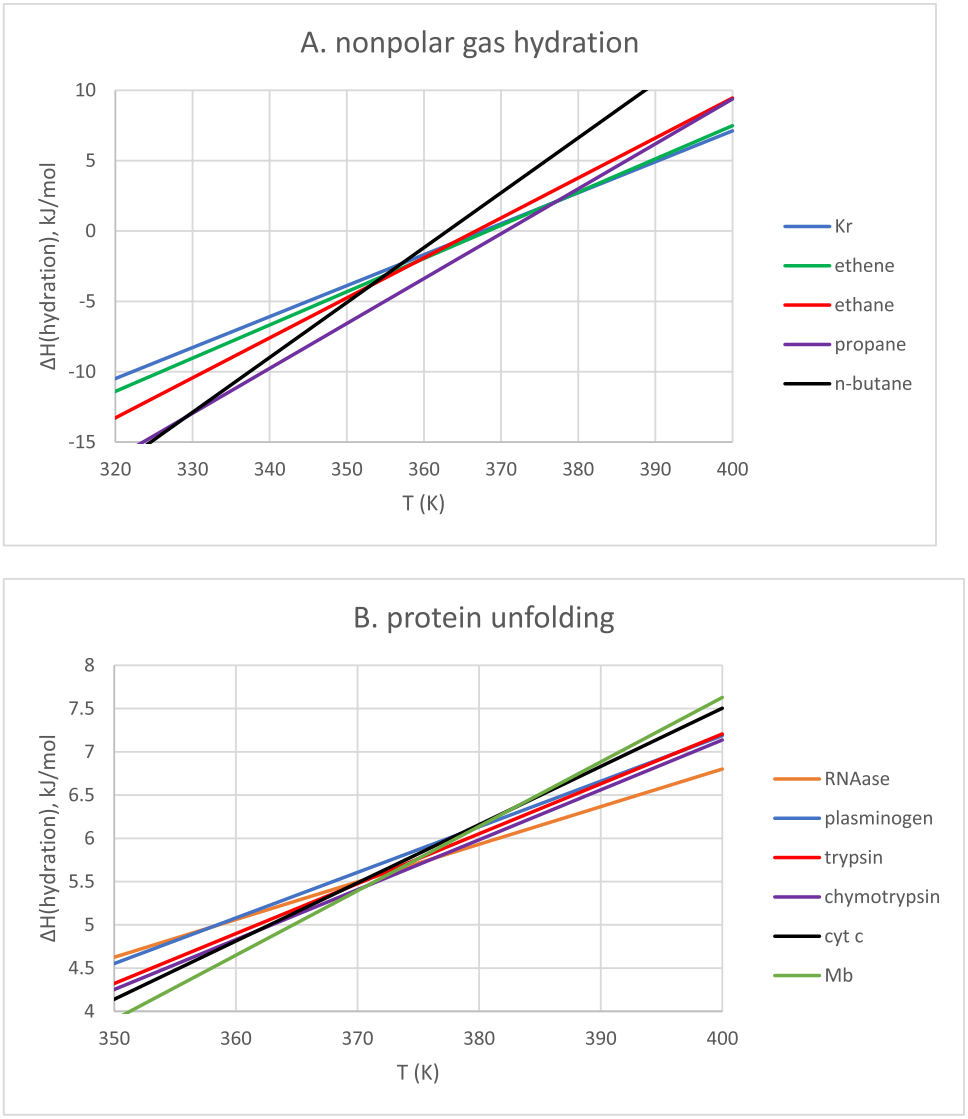

Fig. 14 Temperature dependence of the enthalpy of **a** nonpolar gas hydration, and **b** protein unfolding Data from ref. [101]

to observe convergence behavior in the larger data sets has been recognized by some authors [20], but has been ignored by others [99].

It is important to conclude this discussion by stressing that enthalpy and entropy convergence do not generally exist for protein unfolding, and the existence of enthalpy convergence for hydrophobic hydration can be questioned as well.

Entropy is a measure of freedom of motion

One way to measure entropy is given by Boltzmann's entropy equation,

$$S = R \cdot \ln(W), \tag{22}$$

where R is the gas law constant, 8.314 J/K/mol, and W is the number of ways that a system can be arranged. For an ideal gas, W can be a measure of positions within a volume of space available to the particle. Excluding the particle from a portion of the volume will lower W and thus decrease entropy.

We can demonstrate this by combining the first and second laws of thermodynamics to get, for a fully reversible reaction,

$$\mathrm{d}U(\text{internal energy}) = T \cdot \mathrm{d}S - P \cdot \mathrm{d}V. \tag{23}$$

Furthermore, since $\mathrm{d}U = C_V \cdot \mathrm{d}T$, Eq. (23) becomes

$$\mathrm{d}S = C_V\left(\frac{\mathrm{d}T}{T}\right) + \left(\frac{P}{T}\right)\mathrm{d}V. \tag{24}$$

Using the ideal gas law ($PV = nRT \rightarrow P/T = R/\overline{V}$), we get

$$\mathrm{d}S = C_V\left(\frac{\mathrm{d}T}{T}\right) + R \cdot \frac{\mathrm{d}V}{\overline{V}}. \tag{25}$$

For an isothermal process, $\mathrm{d}T = 0$, so

$$\mathrm{d}S = R \cdot \frac{\mathrm{d}V}{\overline{V}}. \tag{26}$$

For the reversible isothermal compression of an ideal gas, $\mathrm{d}V$ is negative and thus $\mathrm{d}S$ would be negative as well. In other words, restricting the available space curtails freedom of motion, which in turn lowers entropy.

Although the situation is more complex in the liquid (and solid) phase, the general conclusion remains the same: excluding solvent from a volume of space (e.g., a cavity) decreases the entropy of the solvent.

References

1. Silverstein TP (1998) The real reason why oil and water don't mix. J Chem Educ 75:116
2. Solomons TWG, Fryhle CB (2011) Organic chemistry, 10th edn. Wiley, Hoboken, p 81
3. Herzfeld J (1991) Understanding hydrophobic behavior. Science 253:88–89
4. Dill KA, Privalov PL, Gill SJ, Murphy KP (1990) The meaning of hydrophobicity. Science 250:297–299
5. Harris RC, Pettitt BM (2016) Reconciling the understanding of 'hydrophobicity'with physics-based models of proteins. J Phys Condens Matter 28:083003
6. Yaminsky VV, Vogler EA (2001) Hydrophobic hydration. Curr Opin Colloid Interface Sci 6:342–349
7. Baldwin RL (2013) The new view of hydrophobic free energy. FEBS Lett 587:1062–1066
8. Baldwin RL (2012) Gas–liquid transfer data used to analyze hydrophobic hydration and find the nature of the Kauzmann–Tanford hydrophobic factor. Proc Natl Acad Sci 109:7310–7313
9. Baldwin RL (2013) Properties of hydrophobic free energy found by gas–liquid transfer. Proc Natl Acad Sci 110:1670–1673
10. Murphy KP, Privalov PL, Gill SJ (1990) Common features of protein unfolding and dissolution of hydrophobic compounds. Science 247:559–561
11. Dec SF, Gill SJ (1984) Heats of solution of gaseous hydrocarbons in water at 25 °C. J Solut Chem 13:27–41
12. Ben-Amotz D (2016) Water-mediated hydrophobic interactions. Annu Rev Phys Chem 67:617–638
13. Murphy KP (1994) Hydration and convergence temperatures: on the use and interpretation of correlation plots. Biophys Chem 51:311–326
14. Tanford C (1980) Micelles: introduction. In: The hydrophobic effect: formation of micelles and biological membranes, 2nd edn. Wiley, New York, pp 42–58
15. Lucas M, Bury R (1976) The influence of solute size on the thermodynamic parameter of transfer of a nonpolar hydrophobic solute from gas to water or from light to heavy water. J Phys Chem 80:999–1002
16. Chandler D (2005) Interfaces and the driving force of hydrophobic assembly. Nature 437:640–647
17. Lazaridis T, Paulaitis ME (1994) Simulation studies of the hydration entropy of simple, hydrophobic solutes. J Phys Chem 98:635–642
18. Lum K, Chandler D, Weeks JD (1999) Hydrophobicity at small and large length scales. ACS, Washington
19. Ashbaugh HS, Truskett TM, Debenedetti PG (2002) A simple molecular thermodynamic theory of hydrophobic hydration. J Chem Phys 116:2907–2921
20. Ashbaugh HS, Pratt LR (2006) Colloquium: Scaled particle theory and the length scales of hydrophobicity. Rev Mod Phys 78:159
21. Ashbaugh HS (2009) Entropy crossover from molecular to macroscopic cavity hydration. Chem Phys Lett 477:109–111
22. Graziano G (2006) Scaled particle theory study of the length scale dependence of cavity thermodynamics in different liquids. J Phys Chem B 110:11421–11426
23. Hillyer MB, Gibb BC (2016) Molecular shape and the hydrophobic effect. Annu Rev Phys Chem 67:307–329
24. Matulis D, Bloomfield VA (2001) Thermodynamics of the hydrophobic effect. II. Calorimetric measurement of enthalpy, entropy, and heat capacity of aggregation of alkylamines and long aliphatic chains. Biophys Chem 93:53–65
25. Matulis D (2001) Thermodynamics of the hydrophobic effect. III. Condensation and aggregation of alkanes, alcohols, and alkylamines. Biophys Chem 93:67–82
26. Smith R, Tanford C (1973) Hydrophobicity of long chain n-alkyl carboxylic acids, as measured by their distribution between heptane and aqueous solutions. Proc Natl Acad Sci 70:289–293
27. Solomonov BN, Sedov IA (2008) The hydrophobic effect Gibbs energy. J Mol Liq 139:89–97
28. Choudhury N, Pettitt BM (2006) Enthalpy–entropy contributions to the potential of mean force of nanoscopic hydrophobic solutes. J Phys Chem B 110:8459–8463
29. Li IT, Walker GC (2011) Signature of hydrophobic hydration in a single polymer. Proc Natl Acad Sci 108:16527–16532
30. Sharp KA, Madan B (1997) Hydrophobic effect, water structure, and heat capacity changes. J Phys Chem B 101:4343–4348
31. Muller N (1990) Search for a realistic view of hydrophobic effects. Acc Chem Res 23:23–28
32. Lee B, Graziano G (1996) A two-state model of hydrophobic hydration that produces compensating enthalpy and entropy changes. J Am Chem Soc 118:5163–5168
33. Godec A, Merzel F (2012) Physical origin underlying the entropy loss upon hydrophobic hydration. J Am Chem Soc 134:17574–17581
34. Davis JG, Gierszal KP, Wang P, Ben-Amotz D (2012) Water structural transformation at molecular hydrophobic interfaces. Nature 491:582–585
35. Grdadolnik J, Merzel F, Avbelj F (2017) Origin of hydrophobicity and enhanced water hydrogen bond strength near purely hydrophobic solutes. Proc Natl Acad Sci 114:322–327
36. Matysiak S, Debenedetti PG, Rossky PJ (2011) Dissecting the energetics of hydrophobic hydration of polypeptides. J Phys Chem B 115:14859–14865
37. Finney JL, Bowron DT, Daniel RM et al (2003) Molecular and mesoscale structures in hydrophobically driven aqueous solutions. Biophys Chem 105:391–409
38. Silverstein TP, Slade K (2019) Effects of macromolecular crowding on biochemical systems. J Chem Educ 96:2476–2487
39. Ball P (2008) Water as an active constituent in cell biology. Chem Rev 108:74–108
40. Brini E, Fennell CJ, Fernandez-Serra M et al (2017) How water's properties are encoded in its molecular structure and energies. Chem Rev 117:12385–12414
41. Lazaridis T (2001) Solvent size vs cohesive energy as the origin of hydrophobicity. Acc Chem Res 34:931–937
42. Blokzijl W, Engberts JB (1993) Hydrophobic effects. Opinions and facts. Angew Chem Int Ed Engl 32:1545–1579

43. Lucas M (1976) Size effect in transfer of nonpolar solutes from gas or solvent to another solvent with a view on hydrophobic behavior. J Phys Chem 80:359–362
44. Lee B (1991) Solvent reorganization contribution to the transfer thermodynamics of small nonpolar molecules. Biopolym Orig Res Biomol 31:993–1008
45. Pratt LR, Pohorille A (1992) Theory of hydrophobicity: transient cavities in molecular liquids. Proc Natl Acad Sci 89:2995–2999
46. Wallqvist A, Covell DG (1996) On the origins of the hydrophobic effect: observations from simulations of *n*-dodecane in model solvents. Biophys J 71:600–608
47. Durell SR, Wallqvist A (1996) Atomic-scale analysis of the solvation thermodynamics of hydrophobic hydration. Biophys J 71:1695–1706
48. Cerdeiriña CA, Debenedetti PG (2018) Water's thermal pressure drives the temperature dependence of hydrophobic hydration. J Phys Chem B 122:3620–3625
49. Ashbaugh HS, Bukannan H (2020) Temperature, pressure, and concentration derivatives of nonpolar gas hydration: impact on the heat capacity, temperature of maximum density, and speed of sound of aqueous mixtures. J Phys Chem B 124:6924–6942
50. Graziano G (2003) Comment on "A simple molecular thermodynamic theory of hydrophobic hydration"[J. Chem. Phys. 116, 2907 (2002)]. J Chem Phys 119:10448–10449
51. Cabani S, Gianni P, Mollica V, Lepori L (1981) Group contributions to the thermodynamic properties of non-ionic organic solutes in dilute aqueous solution. J Solut Chem 10:563–595
52. Fisicaro E, Compari C, Braibanti A (2004) Entropy/enthalpy compensation: hydrophobic effect, micelles and protein complexes. Phys Chem Chem Phys 6:4156–4166
53. Graziano G (2009) Hydration entropy of polar, nonpolar and charged species. Chem Phys Lett 479:56–59
54. Graziano G (2019) Contrasting the hydration thermodynamics of methane and methanol. Phys Chem Chem Phys 21:21418–21430
55. Edsall JT (1935) Apparent molal heat capacities of amino acids and other organic compounds. J Am Chem Soc 57:1506–1507
56. Silverstein KA, Haymet ADJ, Dill KA (2000) The strength of hydrogen bonds in liquid water and around nonpolar solutes. J Am Chem Soc 122:8037–8041
57. Klotz IM (1958) Protein hydration and behavior. Science 128:815–822
58. Kauzmann W (1959) Some factors in the interpretation of protein denaturation. In: Advances in protein chemistry. Elsevier, Amsterdam, pp 1–63
59. Kozak JJ, Knight WS, Kauzmann W (1968) Solute–solute interactions in aqueous solutions. J Chem Phys 48:675–690
60. Némethy G, Scheraga HA (1962) Structure of water and hydrophobic bonding in proteins. I. A model for the thermodynamic properties of liquid water. J Chem Phys 36:3382–3400
61. Némethy G, Scheraga HA (1962) Structure of water and hydrophobic bonding in proteins. II. Model for the thermodynamic properties of aqueous solutions of hydrocarbons. J Chem Phys 36:3401–3417
62. Tanford C (1962) Contribution of hydrophobic interactions to the stability of the globular conformation of proteins. J Am Chem Soc 84:4240–4247
63. Tanford C (1978) The hydrophobic effect and the organization of living matter. Science 200:1012–1018
64. Hildebrand JH (1979) Is there a "hydrophobic effect"? Proc Natl Acad Sci USA 76:194
65. Gill SJ, Dec SF, Olofsson G, Wadsö I (1985) Anomalous heat capacity of hydrophobic solvation. J Phys Chem 89:3758–3761
66. Head-Gordon T (1995) Is water structure around hydrophobic groups clathrate-like? Proc Natl Acad Sci 92:8308–8312
67. Xu H, Dill K (2005) Water's hydrogen bonds in the hydrophobic effect: a simple model. J Phys Chem B 109:23611–23617
68. Rezus YLA, Bakker HJ (2007) Observation of immobilized water molecules around hydrophobic groups. Phys Rev Lett 99:148301
69. Irudayam SJ, Henchman RH (2010) Solvation theory to provide a molecular interpretation of the hydrophobic entropy loss of noble-gas hydration. J Phys: Condens Matter 22:284108
70. Ashbaugh HS, Barnett JW, Saltzman A et al (2016) Communication: stiffening of dilute alcohol and alkane mixtures with water. J Chem Phys 145:201102
71. Wu X, Lu W, Streacker LM et al (2018) Methane hydration-shell structure and fragility. Angew Chem Int Ed 57:15133–15137
72. Galamba N (2013) Water's structure around hydrophobic solutes and the iceberg model. J Phys Chem B 117:2153–2159
73. Baldwin RL (2014) Dynamic hydration shell restores Kauzmann's 1959 explanation of how the hydrophobic factor drives protein folding. Proc Natl Acad Sci 111:13052–13056
74. Meister K, Strazdaite S, DeVries AL et al (2014) Observation of ice-like water layers at an aqueous protein surface. Proc Natl Acad Sci 111:17732–17736
75. Brotzakis ZF, Voets IK, Bakker HJ, Bolhuis PG (2018) Water structure and dynamics in the hydration layer of a type III antifreeze protein. Phys Chem Chem Phys 20:6996–7006
76. Kim J, Tian Y, Wu J (2015) Thermodynamic and structural evidence for reduced hydrogen bonding among water molecules near small hydrophobic solutes. J Phys Chem B 119:12108–12116
77. Graziano G (2014) Comment on "Water's structure around hydrophobic solutes and the Iceberg Model". J Phys Chem B 118:2598–2599
78. Dec SF, Bowler KE, Stadterman LL et al (2006) Direct measure of the hydration number of aqueous methane. J Am Chem Soc 128:414–415
79. Buchanan P, Aldiwan N, Soper AK et al (2005) Decreased structure on dissolving methane in water. Chem Phys Lett 415:89–93
80. Kinoshita M (2008) Molecular origin of the hydrophobic effect: analysis using the angle-dependent integral equation theory. J Chem Phys 128:01B612
81. Islam N, Flint M, Rick SW (2019) Water hydrogen degrees of freedom and the hydrophobic effect. J Chem Phys 150:014502
82. Bergman DL, Lynden-Bell RM (2001) Is the hydrophobic effect unique to water? The relation between solvation properties and network structure in water and modified water models. Mol Phys 99:1011–1021
83. Lee B (1994) Enthalpy-entropy compensation in the thermodynamics of hydrophobicity. Biophys Chem 51:271–278
84. Madan B, Lee B (1994) Role of hydrogen bonds in hydrophobicity: the free energy of cavity formation in water models with and without the hydrogen bonds. Biophys Chem 51:279–289
85. Bernal JD (1939) Structure of proteins. Nature 143:663–667
86. Dill KA (1990) Dominant forces in protein folding. Biochemistry 29:7133–7155
87. Livingstone JR, Spolar RS, Record MT Jr (1991) Contribution to the thermodynamics of protein folding from the reduction in water-accessible nonpolar surface area. Biochemistry 30:4237–4244
88. Pace CN, Fu H, Fryar KL et al (2011) Contribution of hydrophobic interactions to protein stability. J Mol Biol 408:514–528
89. Pace CN, Shirley BA, McNutt M, Gajiwala K (1996) Forces contributing to the conformational stability of proteins. FASEB J 10:75–83
90. Harano Y, Kinoshita M (2005) Translational-entropy gain of solvent upon protein folding. Biophys J 89:2701–2710
91. Lesser GJ, Rose GD (1990) Hydrophobicity of amino acid subgroups in proteins. Proteins Struct Funct Bioinform 8:6–13
92. Li L, Li C, Zhang Z, Alexov E (2013) On the dielectric "constant" of proteins: smooth dielectric function for macromolecular modeling and its implementation in DelPhi. J Chem Theory Comput 9:2126–2136

93. Rees DC, Robertson AD (2001) Some thermodynamic implications for the thermostability of proteins. Protein Sci 10:1187–1194
94. Pica A, Graziano G (2016) Shedding light on the extra thermal stability of thermophilic proteins. Biopolymers 105:856–863
95. Graziano G (2014) On the mechanism of cold denaturation. Phys Chem Chem Phys 16:21755–21767
96. Graziano G (2015) The Gibbs energy cost of cavity creation depends on geometry. J Mol Liq 211:1047–1051
97. Graziano G (2019) Some clues on the conformational stability of globular proteins. Trends Pept Protein Sci 4:1–1
98. Graziano G (2008) Is there a relationship between protein thermal stability and the denaturation heat capacity change? J Therm Anal Calorim 93:429–438
99. Sawle L, Ghosh K (2011) How do thermophilic proteins and proteomes withstand high temperature? Biophys J 101:217–227
100. Razvi A, Scholtz JM (2006) A thermodynamic comparison of HPr proteins from extremophilic organisms. Biochemistry 45:4084–4092
101. Privalov PL, Gill SJ (1988) Stability of protein structure and hydrophobic interaction. In: Advances in protein chemistry. Elsevier, Amsterdam, pp 191–234
102. Robertson AD, Murphy KP (1997) Protein structure and the energetics of protein stability. Chem Rev 97:1251–1268
103. Seong S-Y, Matzinger P (2004) Hydrophobicity: an ancient damage-associated molecular pattern that initiates innate immune responses. Nat Rev Immunol 4:469–478
104. Ohtaka H, Schön A, Freire E (2003) Multidrug resistance to HIV-1 protease inhibition requires cooperative coupling between distal mutations. Biochemistry 42:13659–13666
105. Biela A, Sielaff F, Terwesten F et al (2012) Ligand binding stepwise disrupts water network in thrombin: enthalpic and entropic changes reveal classical hydrophobic effect. J Med Chem 55:6094–6110
106. Fernández-Vidal M, White SH, Ladokhin AS (2011) Membrane partitioning: "classical" and "nonclassical" hydrophobic effects. J Membr Biol 239:5–14
107. Ross PD, Subramanian S (1981) Thermodynamics of protein association reactions: forces contributing to stability. Biochemistry 20:3096–3102
108. Bingham RJ, Findlay JB, Hsieh S-Y et al (2004) Thermodynamics of binding of 2-methoxy-3-isopropylpyrazine and 2-methoxy-3-isobutylpyrazine to the major urinary protein. J Am Chem Soc 126:1675–1681
109. Meyer EA, Castellano RK, Diederich F (2003) Interactions with aromatic rings in chemical and biological recognition. Angew Chem Int Ed 42:1210–1250
110. Syme NR, Dennis C, Phillips SE, Homans SW (2007) Origin of heat capacity changes in a "nonclassical" hydrophobic interaction. ChemBioChem 8:1509–1511
111. Setny P, Baron R, McCammon JA (2010) How can hydrophobic association be enthalpy driven? J Chem Theory Comput 6:2866–2871
112. Privalov PL (1979) Stability of proteins small globular proteins. In: Advances in protein chemistry. Elsevier, Amsterdam, pp 167–241
113. Ben-Naim A (1978) Standard thermodynamics of transfer. Uses and misuses. J Phys Chem 82:792–803
114. Murphy KP, Gill SJ (1990) Group additivity thermodynamics for dissolution of solid cyclic dipeptides into water. Thermochim Acta 172:11–20
115. Murphy KP, Gill SJ (1991) Solid model compounds and the thermodynamics of protein unfolding. J Mol Biol 222:699–709
116. Baldwin RL (1986) Temperature dependence of the hydrophobic interaction in protein folding. Proc Natl Acad Sci 83:8069–8072
117. Garde S, Hummer G, Garcia AE et al (1996) Origin of entropy convergence in hydrophobic hydration and protein folding. Phys Rev Lett 77:4966
118. Lee B, Richards FM (1971) The interpretation of protein structures: estimation of static accessibility. J Mol Biol 55:379–384
119. Chothia C (1984) Principles that determine the structure of proteins. Annu Rev Biochem 53:537–572
120. Bello J (1978) Tight packing of protein cores and interfaces: relation to conservative amino acid sequences and stability of protein–protein interaction. Int J Pept Protein Res 12:38–41
121. Huang DM, Chandler D (2000) Temperature and length scale dependence of hydrophobic effects and their possible implications for protein folding. Proc Natl Acad Sci 97:8324–8327